





# Water Resources Research<sup>®</sup>



## RESEARCH ARTICLE

10.1029/2020WR029362

# Consequences of Dryland Maize Planting Decisions Under Increased Seasonal Rainfall Variability

N. T. Krell<sup>1</sup> , B. E. Morgan<sup>1</sup> , D. Gower<sup>2</sup> , and K. K. Caylor<sup>1,3</sup> 

<sup>1</sup>Department of Geography, University of California, Santa Barbara, CA, USA, <sup>2</sup>Earth System Science Interdisciplinary Center, University of Maryland, College Park, MD, USA, <sup>3</sup>Bren School of Environmental Science and Management, University of California, Santa Barbara, CA, USA

### Key Points:

- Small-scale rainfed maize production is highly susceptible to climate variability
- Maize variety choice determines potential yield but also changes exposure to dry periods
- Nonlinearities between seasonal rainfall, yield, and rainfall statistics lead to divergent outcomes

### Correspondence to:

N. T. Krell,  
nkrell@ucsb.edu

### Citation:

Krell, N. T., Morgan, B. E., Gower, D., & Caylor, K. K. (2021). Consequences of dryland maize planting decisions under increased seasonal rainfall variability. *Water Resources Research*, 57, e2020WR029362. <https://doi.org/10.1029/2020WR029362>

Received 10 DEC 2020

Accepted 13 AUG 2021

**Abstract** Shifts in rainfall frequency and intensity can lead to heavy crop loss in rainfed agricultural systems. Small-scale farmers who plant with limited resources need to carefully select management strategies that are well suited for their environment. Farmers must choose between planting higher-yielding varieties that take longer to mature and lower-yielding varieties that can be harvested sooner. To better understand the interactions between rainfall variability, cultivar choice, and cropping success, we implement an ecohydrological model that accounts for variation in daily soil moisture and converts water stress to crop yield. We apply the model to growing conditions of dryland farmers in central Kenya, which is a drought-prone and semiarid region with spatially heterogeneous rainfall. To simulate stochastic daily rainfall, we derive parameters in 10-day increments from a 30+ year daily rainfall data set. We use these properties to model the stochastic seasonal water availability for cultivars with different maturation lengths. In agreement with past studies, our analysis shows that storms are becoming more intense and less frequent. We show that maize crops are prone to water deficit in the part of the growing season when crop water requirements are highest. Despite the potential for higher-yielding, late maturing varieties to improve total harvest, we find that early maturing varieties that are drought-avoidant have the lowest likelihood of failure. In light of reduced rainfall totals, we show that the historical probability of crop failure was lowest in the past and is now increasing.

## 1. Introduction

In semiarid and arid regions of sub-Saharan Africa rising temperatures and shifting rainfall patterns are projected to negatively impact agricultural output (Downing et al., 1997; Branca et al., 2011; Müller et al., 2011; Slingo et al., 2005). Changes in rainfall associated with climate variability directly impact crop growth as storms are projected to become more intense with longer periods between rainfall events (Donat et al., 2016; Harrison et al., 2019; Meehl et al., 2007). The stochastic nature of rainfall during the growing season leaves crops susceptible to water stress during critical stages of development and can lead to crop failure (Sah et al., 2020; Salgado-Aguilar et al., 2020). Small rainfed farms cultivated by single families on plots less than 5 ha represent the most prevalent form of agriculture in sub-Saharan Africa and are particularly vulnerable to climate variability and change (Samberg et al., 2016). Because of their dependence on rainfed agriculture (Dinar et al., 2008), smallholder livelihoods are susceptible to climate shocks that affect food prices (Ray et al., 2012), variability in production and supply (Lobell et al., 2011; Slingo et al., 2005), and farmer incomes (Reidsma et al., 2010).

Farmers make a variety of choices before and during the growing season that impact their agricultural production and thus food security and livelihood. Cultivar choice is one of the most critical choices a smallholder makes (Kalanda-Joshua et al., 2011). Because of the uncertainty associated with climate variability, farmer decision-making is becoming increasingly complex and uncertain at the expense of input use efficiency and profitability (Hansen et al., 2011; Guido et al., 2020; Waldman et al., 2019). Management options that were optimal for past or average climatic conditions may no longer be suited for increasingly common growing season weather. Additionally, traditional crop varieties may no longer be best suited for a farmer's environment, which has led to the development of hybrid and fast growing varieties (Smale & Jayne, 2010). Given ongoing changes in rainfall patterns, farmers need to select cultivars well suited for their local context that can lead to the greatest payoff in terms of yield while also minimizing the risk of crop failure. To date,

© 2021. The Authors.

This is an open access article under the terms of the [Creative Commons Attribution License](https://creativecommons.org/licenses/by/4.0/), which permits use, distribution and reproduction in any medium, provided the original work is properly cited.

however, no modeling exercise to understand the effect of stochastic rainfall variability on maize yields for various cultivars exists for dryland environments in sub-Saharan Africa.

To evaluate the impact of farmer decision-making and climate variability on agricultural outcomes, both field and modeling approaches have been employed (e.g., Bharwani et al., 2005; Choi et al., 2015; Roudier et al., 2014; Vervoort et al., 2016; Wood et al., 2014; Ziervogel et al., 2005). While field studies provide empirical evidence of environmental impacts on farmer outcomes, they can be limited to certain conditions, especially when panel data are absent (Hansen et al., 2011; Patt et al., 2005) and are difficult to extrapolate to scenarios where the climate is changing. Alternatively, crop models can be useful when field data are unavailable, but such models can also be limited in applicability and need to be carefully parameterized with special attention to how stochastic rainfall is modeled. However, given that daily rainfall observations with long temporal extents are generally unavailable for rainfed agricultural systems it is difficult to robustly estimate rainfall parameters. In rainfed contexts, variability in inter- and intra-annual rainfall is closely linked to variability in production. Crop models and agronomic studies in general focus on annual, seasonal or monthly rainfall totals (Barron et al., 2003) and do not provide a much-needed evaluation of interannual variability of within-season dynamics, which has important implications for crop yields (Recha et al., 2012). Dryland regions in particular necessitate careful modeling of rainfall patterns that are heterogeneous in space and time. An improved understanding of rainfall variability considers the temporal distribution of rainfall through analyses of the average amount of rain during rainfall events and the average length of time between successive events (Recha et al., 2012).

In order to develop a better way to study these systems, two concerns must be addressed. First a more accurate consideration of rainfall dynamics in semiarid environments is needed. Considering the stochastic nature of rainfall rather than the seasonal averages is important in these systems where the frequency and duration of rainfall lead to important consequences for vegetation response (Katul et al., 2007; Porporato et al., 2002). Localized convective storms arrive in pulses that beget nonlinear vegetation response (Baude-na et al., 2007; Katul et al., 2007). Second, in addition to considerations of the hydroclimatic environment, the representation of vegetation needs to be specific to a crop of interest. While researchers have separately undertaken modeling exercises to understand the impact of climate variability on crop growth and the stochastic nature of rainfall on vegetation structure, there have been fewer efforts to link stochastic rainfall dynamics to the probability of crop failure for staple crops such as maize. Specifically, understanding the influence of cultivar choice on the success of a crop has not been considered.

This study is motivated by the need to better understand the coupled dynamics of water and rainfed agricultural systems in dryland regions occupied by smallholder farmers. In general, the relationship between soil moisture and maize yields is poorly resolved (Rigden et al., 2020). We address this need by presenting a model of stochastic seasonal soil water availability that evaluates the impacts of intra-seasonal rainfall variability on crop production in a smallholder agricultural system. This model is based on a previously explored stochastic soil water balance model (Laio et al., 2001; Laio, Porporato, Fernandez-Illescas, & Rodríguez-Iturbe, 2001; Porporato et al., 2001; Rodríguez-Iturbe et al., 2001) that simulates the interactions between soil, plants, and climate. The point-based model is nonspatial and determines daily growing and harvest season values of runoff, interception, leakage and evapotranspiration for a given soil type and cultivar. Rainfall is represented as a marked Poisson process expressed as the mean depth of daily rainfall and the mean probability of storm arrival, which forces the model at the daily time step.

We apply this model to a study site in central Kenya that exhibits a high degree of rainfall variability. Using a long-term daily precipitation data set and a characteristic soil type for the region we estimate climate and soil parameters for the model. We use the stochastic soil water balance model to determine yield outcomes and the probability of crop failure, which are a function of plant water deficit (dynamic water stress). We compare and evaluate our model results for various maize varieties with late, medium and early harvesting periods. We aim to answer the following questions for our study area:

1. What do historical records (40+ years) indicate about interannual rainfall trends?
2. How does intra-seasonal rainfall variability interact with the static and dynamic stress of a maize crop?
3. How do varying maize cultivars moderate the effect of climate variability on changes in yields and crop failure?
4. Has the average yield of maize production and likelihood of crop failure changed over an 80 year period?

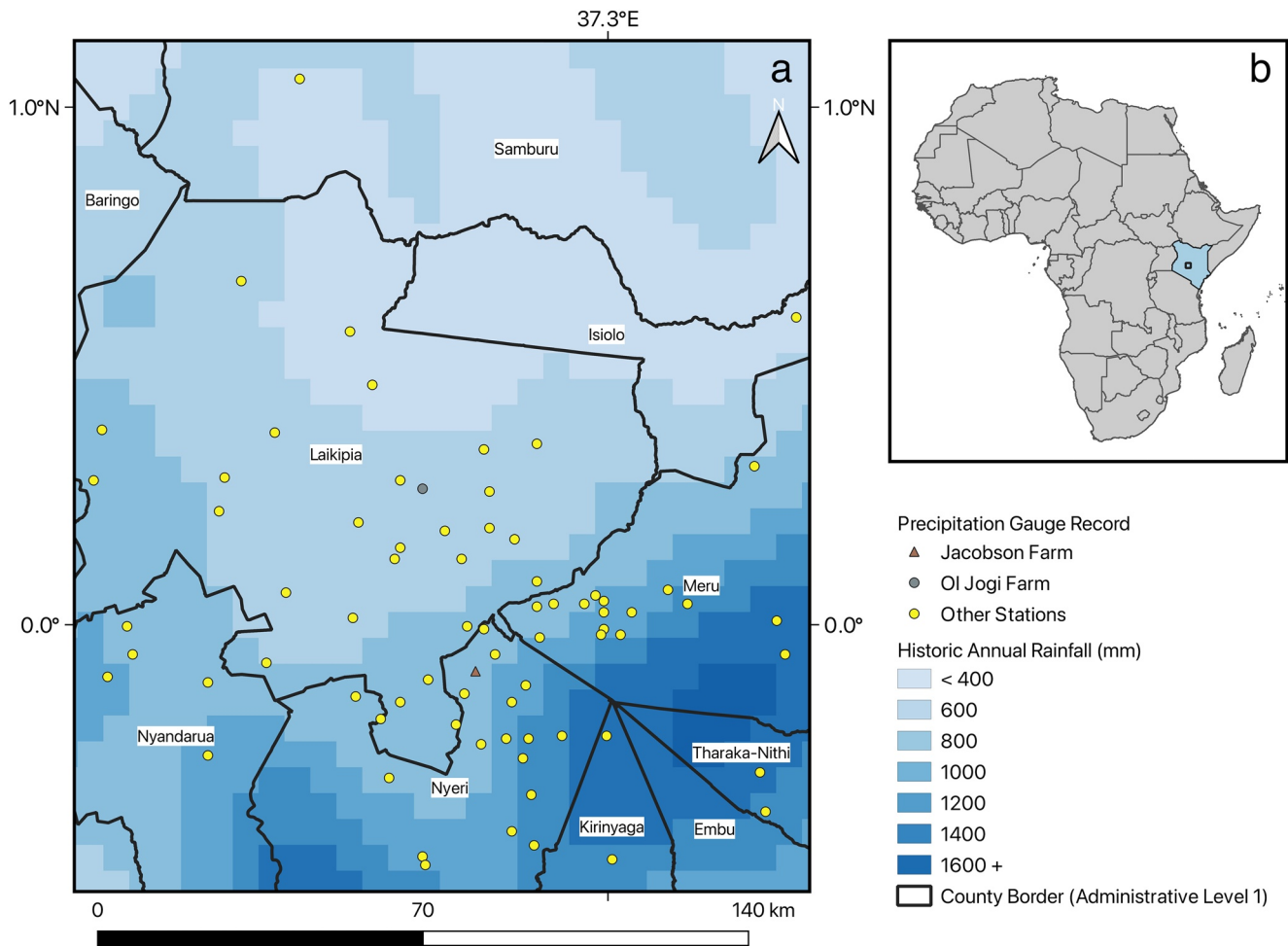


**Figure 1.** Maps showing: (a) Inset of study site within central Kenya; (b) Study site in Kenya noted by black box. Point data is from 80 stations. Jacobson Farm and Ol Jogi Farm are denoted with a triangle and circle icon, respectively. Shades of blue indicate historic annual rainfall based on enhanced Climate Hazards Group InfraRed Precipitation with Station (CHIRPS) data that was created by blending 710 quality controlled station observations with the publicly available CHIRPS product averaged over 10-day periods in 1983–2016. Contours were delineated using the GeoClim Contour Tool using an interval of 200 mm.

The following paper is organized as follows: We first describe our study site and the hydro-meteorological data necessary to apply the soil water balance model in the methods section. We then introduce our modeling framework and metrics for converting stress into yield. Our results demonstrate the impact of intra-seasonal rainfall variability on the seasonal water availability of maize varieties. We discuss these findings in the context of smallholder farmer decision-making and explore the implications of the results in the context of historical trends in rainfall and thus crop failure. We conclude with a discussion of model limitations and suggest additional research agendas appropriate for our proposed model.

## 2. Methods

### 2.1. Study Site

We apply our model to the smallholder farming communities on the western slope of Mount Kenya, specifically the Laikipia plateau, in East Africa shown in Figure 1. Laikipia county is located on the western (lee-ward) side of Mount Kenya and is adjacent to Meru and Nyeri counties in central Kenya. The county comprises smallholder agriculturalists, growing urban areas, and wildlife conservatories that attract tourism. The presence of dryland agriculturalists along a heterogeneous rainfall gradient makes the area suitable for an analysis of rainfall variability and cropping outcomes. The main cropping season for maize is planting around day 100 (first week of April) and harvesting around day 300 (last week of October) (Ray et al., 2015).

**Table 1**  
Parameters Associated With Three Prominent Soil Textures Found Within the Study Site

Soil type	$\Psi_s$ (MPa) <sup>b</sup>	$b^b$	$K_s$ (cm/d) <sup>b</sup>	$n^b$	$s_h$	$s_{fc}$
Clay	$-3.97 \times 10^{-3}$	11.4	11.1	0.482	0.503	0.830
Clay loam	$-6.17 \times 10^{-3}$	8.52	21.2	0.476	0.420	0.821
Sandy clay loam	$-2.93 \times 10^{-3}$	7.12	54.4	0.420	0.319	0.711

<sup>a</sup>We calculated values of  $s_h$  and  $s_{fc}$  assuming a soil water potential  $\Psi_h = -10.0$  MPa and  $\Psi_{sfc} = -0.03$  MPa (Laio et al., 2001). <sup>b</sup>Clapp and Hornberger (1978).

Laikipia is a semiarid region prone to severe water deficits due to unreliable rainfall and high spatial and temporal variability. Rainfall in Kenya is characterized by a high coefficient of variability, which is common to semiarid environments (Herrero et al., 2010). Furthermore, Laikipia has a heterogeneous landscape and complex topography that results in a rainfall gradient. While the foothills of Mount Kenya often receive between 800 and 900 mm of rainfall annually, the northern end of the county receives less than 500 mm annually (Wiesmann, 1998). The annual distribution of rainfall is bimodal with two rainy seasons: the long (roughly March through May) and short (roughly October through December) rains.

The Laikipia region of Kenya serves as an ideal study site to model the relationships between smallholder agriculture and climate variability for two reasons: (a) the tight couplings between food production and rainfall and (b) the prevalence of maize cultivation under various rainfall climatologies. In the region's drylands smallholder farmers face considerable challenges as rainfall arrives in pulses and in limited quantities for the majority of the year. Because the country has experienced a number of droughts in recent years, the Government of Kenya is especially interested in drought mitigation and increasing food security (Government of Kenya, 2010). Maize is an appropriate crop to study because it is grown under rainfed conditions and is an annual crop subject to both intermittent and terminal drought. Intermittent drought is caused by finite periods of inadequate water availability which does not necessarily result in crop failure whereas terminal drought is a progressive reduction in water availability that leads to crop failure before the end of the growing season (Neumann, 2008).

### 2.1.1. Soil Types

We use the ISRIC Africa SoilGrids soil data base (Leenaars, 2014) to determine the soil textures found at depth 5–15 cm in our study site (Figure 1). The region has a heterogeneous mix of soil textures. The most prevalent soil textures, at the points of the rainfall gauges, are clay, clay loam, and sandy clay loam. Soils in our catchment are geologically young soils derived from basaltic volcanic rock and are generally fertile but susceptible to erosion. The clay soils have high water storage capacities, which can be suitable for growing maize (Muchena & Gachene, 1988). In Table 1 we show the corresponding values for the soil matrix potential at the hygroscopic point  $\Psi_{s_h}$ , and at field capacity  $\Psi_{s_{fc}}$ , the porosity  $n$ , and the saturated hydraulic conductivity  $K_s$  according to the values found in Clapp and Hornberger (1978).

### 2.1.2. Interannual Trends in Long-Term Rainfall Records

To assess whether interannual trends are changing across Laikipia, we use long-term records of daily rainfall data for stations across the study site provided by the Centre for Training and Integrated Research in Arid and Semi-Arid Lands Development (CETRAD) in Nanyuki, Kenya. The gauges, shown in Figure 1, have record lengths between 7 and 79 years. For computing statistics in Table 4, we used stations with records of 40+ years. We considered temporal trends in the two parameters: the average depth per rain event ( $\alpha$ ) and the average rain event frequency per day ( $\lambda$ ) during the two rainy seasons: long (March–May) and short (October–December) rains. We used these daily records to calculate mean rain depth per event ( $\alpha$ ), and rain event frequency ( $\lambda$ ), values for the regional trend analysis shown in Table 4, which is different than the calculation of 10-day estimates of rain depth and rain event frequency described in Section 2.2.1.1 and used for the model parameters.

To analyze interannual trends in the total seasonal rainfall, rain depth per event and rain event frequency parameters for the two seasons, we used a modified Mann-Kendall statistical test and the Theil-Sen

estimator. We use a variance corrected Mann-Kendall test proposed by Yue and Wang (2004), which is appropriate for rainfall data and calculates an effective sample size using the lag-1 autocorrelation coefficient. We used the modified-mk package in R (Patakamuri & O'Brien, 2020).

### 2.1.3. Maize Varieties and Yields

In addition to being a function of environmental conditions and management decisions, total yields also depend on the maize variety. To define maximum potential yields for our simulations, we use empirical yield potentials for maize varieties typically grown by smallholder farmers in Laikipia. These data were sourced from Kenya Seed Company (see Figure 3). The gap between yields reported by seed companies which were grown under controlled conditions and on small-scale farmers' fields is likely greatest in sub-Saharan Africa compared to other regions (Setimela et al., 2017). Evidence from Zambia shows that yields attained by seed companies in optimal settings and the actual realized yields by small-scale farmers can be vastly different (Blekking et al., 2021). Thus, the values of yields used in our model should be considered as the "potential" yield attained by farmers rather than what is realized in-field. We discuss the uncertainty between these measures in Appendix A. We use the linear regression trend to set maximum potential yields for a range of maize varieties with maturity periods between 80 and 180 days, which is further discussed in Section 2.3.1. For each maize variety, we calculate a maximum potential yield,  $Y_{max}$ , which is used in Equation 17.

## 2.2. Model Description

### 2.2.1. Hydrological Water Balance

To characterize the field-scale water balance we use a simple single-layer model of soil moisture at a point. The overall water balance is given by:

$$nZ_r \frac{ds(t)}{dt} = R(t) - I(t) - ET(s(t)) - L(s(t)) - Q(s(t)), \quad (1)$$

where  $n$  is porosity [-],  $Z_r$  is the rooting depth [mm],  $s(t)$  is the saturation, or relative soil moisture content ( $0 \leq s(t) \leq 1$ ),  $R(t)$  is the rainfall rate [mm day<sup>-1</sup>],  $I(t)$  is the amount of rainfall lost through canopy interception [mm day<sup>-1</sup>],  $E(s(t))$  is the rate of evapotranspiration [mm day<sup>-1</sup>],  $L(s(t))$  is the rate of leakage [mm day<sup>-1</sup>], and  $Q(s(t), t)$  is the runoff rate [mm day<sup>-1</sup>]. This is analogous to Equation 1 from Rodriguez-Iturbe et al. (2001).

#### 2.2.1.1. Rainfall

How rainfall varies within seasons and between seasons is highly important to dryland agriculturalists, and we capture both of these aspects of rainfall variability in our model. First, we wanted to capture the within seasonal variability of rainfall, which we model using two parameters: the average depth per rain event,  $\alpha$  and the rain event frequency,  $\lambda$ . Rainfall is treated as a time-varying marked Poisson process. In each 10-day increment  $i$ , rainfall occurs with a probability,  $\lambda_i$  [day<sup>-1</sup>], and the depth of rainfall events are drawn from an exponential distribution with a mean value,  $\alpha_i$  [mm]. Values of  $\lambda$  and  $\alpha$  used to model daily rainfall are estimated over 10-day fixed window intervals from a long-term rainfall record of daily station rainfall data, which was described previously in Section 2.1.2. To capture the seasonal variation in rainfall parameters, we selected a 10-day fixed window instead of monthly intervals to estimate  $\alpha$  and  $\lambda$ , which are then used to simulate daily rainfall during the season. The choice of a 10-day interval allowed rainfall parameters to vary within each month, which is important for capturing the onset and end of the rainy seasons in this region. However, even with multiple decades of data (e.g., 31 years of data at the Ol Jogi station), there are not enough observations of rainfall to justify daily parameter estimates.

Second, we wanted to model the interannual variability of total seasonal amounts in a way that most closely represented observations from our rain gauge record. It is well documented that simple stochastic models fitted to daily rainfall data tend to underestimate the variance of precipitation at longer time intervals thus leading to overdispersion (e.g., Katz & Parlange, 1998). We found that using a fixed rainfall climatology across seasons led to underestimations of the variance in seasonal rainfall from year-to-year and did not accurately represent the observed coefficient of variation in seasonal rainfall for our rain gauge locations of interest. Many approaches have been introduced to better reproduce the rainfall process and preserve

both the variance observed in the underlying data and intra-annual precipitation statistics (e.g., Fatichi et al., 2011).

As described earlier, our intraseasonal estimates of  $\lambda$  and  $\alpha$  are average values derived from multi-year averages of the rainfall process for each 10-day interval. However it is likely that inherent variability in these parameters from year-to-year leads to increased variance in seasonal totals compared to what we see when using the same average values for each season. To account for this additional variability in the rainfall process between seasons, we modify all of the 10-day  $\lambda$  increments for each season of our simulation using multiplicative Gaussian noise. Specifically, for each season, we multiply the original  $\lambda_i$  for each 10-day time interval by the same seasonal scale factor, which is drawn randomly for each season from a normal distribution with a mean of 1 and a standard deviation of 0.35. The scale factor of 0.35 was selected in order to match the coefficient of variation and seasonal totals from the OI Jogi and Jacobson Farm stations. We recognize that there are many possible mechanisms that could increase the variability of seasonal rainfall totals and that some of these mechanisms would be tied to the daily rainfall process itself in ways that would require modification of the time-varying Poisson model we have proposed. However, the addition of the random multiplicative noise offers a simple approach for capturing interseasonal variability in rainfall without making additional and more complex assumptions regarding the probabilistic nature of the daily rainfall process.

### 2.2.1.2. Interception and Evapotranspiration

In maize systems, rainfall interception by the canopy is proportional to canopy Leaf Area Index (LAI) and will therefore be highest during tasseling (reproductive) and maturity stages (Zheng et al., 2018). We included a simple estimate of interception  $I(t)$  such that

$$I(t) = LAI^* I_e \quad (2)$$

where the crop  $LAI$ , defined in Equation 5, is transformed linearly by an interception efficiency term  $I_e$  [ $\text{mm LAI}^{-1}$ ] which converts the units of  $LAI$  to canopy interception [ $\text{mm day}^{-1}$ ].  $I_e$  is also known as the specific interception capacity and has been previously shown to be between 0.1 and 0.4 in Mahfouf and Jacquemin (1989). We selected a value of 1 for  $I_e$ , which allows for maximum of 3 mm of canopy interception per day. Although this interception efficiency term is seemingly high, we find that this leads to comparable canopy loss compared to other studies. Zheng et al. (2018) found that canopy interception loss accounted for ~12 percent of gross rainfall in a semiarid region in China. In our model, we found that the average seasonal interception was 45 mm and also roughly 12 percent of gross rainfall (355 mm).

Evapotranspiration depends on both the soil moisture,  $s$ , and the time into the growing season,  $t$ . We separate evapotranspiration into its two components, soil evaporation  $E(s, t)$  and plant transpiration  $T(s, t)$  such that

$$ET(s, t) = E(s, t) + T(s, t). \quad (3)$$

Soil evaporation depends on both the amount of soil moisture and the extent of the crop canopy, which intercepts radiation and reduces energy available for soil evaporation. We define evaporation as

$$E(s, t) = \begin{cases} 0 & 0 \leq s < s_h \\ \left( \frac{s - s_h}{1 - s_h} \right)^{q_e} ET_{\max} e^{-0.5 \cdot LAI(t)} & s_h \leq s \leq 1 \end{cases}, \quad (4)$$

where  $q_e$  represents the non-linear rate at which soil evaporation declines as soil moisture drops below saturation,  $LAI$  denotes the crop  $LAI$  [ $\text{mm}^2 \text{mm}^{-2}$ ], a measure of canopy density, and  $s_h$  is the soil moisture at the hygroscopic point.  $ET_{\max}$  is both the maximum  $PET$  and maximum bare soil evaporation.  $LAI(t)$  varies depending on the time into the growing season,  $t$ , and is calculated from the maximum  $LAI$  of a given crop,  $LAI_{c, \max}$  and the crop coefficient,  $K_c(t)$ , as follows:

$$LAI(t) = K_c(t) \left( \frac{LAI_{c, \max}}{K_{c, \max}} \right)^p \quad (5)$$

which assumes a linear relationship between  $LAI$  and  $K_c$  ( $p = 1$ ). We use a convex function of soil moisture for evaporation because with a 400 mm depth uniform layer we cannot easily resolve the problem of different evaporation curves for a two layer model. Rather, we consider that evaporation drops off relatively

fast below saturation and thus we might be under estimating evaporation in certain cases such as in large rainfall events early in the season or when the soil is very wet, which is a method applied in previous studies (e.g., Caylor et al., 2005; Porporato et al., 2003). Future research could employ a more mechanistic approach to resolve Stage 1 and Stage 2 evaporation processes.

### 2.2.1.3. Seasonal Variation in the Crop Coefficient

We use crop coefficient ( $K_c$ ) values based on those listed in FAO guidelines for 180-day maize (grain) in high altitude East Africa, which are defined as 0.3, 0.3, 1.2, 1.2, and 0.6 and correspond to 0%, 16%, 44%, 76%, and 100% of the growing season (Allen et al., 1998). We selected this metric for  $K_c$  because it is widely used in the Crop Water Requirement Satisfaction Index (Senay, 2004) when locally appropriate values are absent. The growing season is divided into four stages of crop phenology, through which the crop coefficient varies, peaking in mid-season after the reproductive stage. The crop coefficient is determined as

$$K_c(t) = \begin{cases} K_{c,ini} & t \leq f_i \\ \frac{K_{c,max} - K_{c,ini}}{f_d - f_i}(t - f_i) + K_{c,ini} & f_i < t \leq f_d \\ K_{c,max} & f_d < t \leq f_{ms} \\ \frac{K_{c,eos} - K_{c,max}}{f_{ls} - f_{ms}}(t - f_{ms}) + K_{c,max} & f_{ms} < t < f_{ls} \\ K_{c,eos} & t = f_{ls} \end{cases} \quad (6)$$

where  $f_i$ ,  $f_d$ ,  $f_{ms}$ , and  $f_{ls}$  denote the fraction of the growing season in days from the beginning of the growing season to the vegetative period (initial), reproductive period (development), maturity period (mid-season), and end of season (late season), respectively. The values of  $K_c$  during vegetative and maturity periods are constant functions of time and the values of  $K_c$  during reproductive and senescence stages are linearly interpolated between the values for the start and end of each period.

The rate of plant transpiration,  $T(s)$ , is given as

$$T(s) = \begin{cases} 0 & s < s_w \\ \frac{s - s_w}{s^* - s_w} K_c T_{max} & s_w \leq s < s^* \\ K_c T_{max} & s^* \leq s \leq 1 \end{cases} \quad (7)$$

where  $T_{max}$  is the maximum transpiration rate of the plant,  $s_w$  is the soil moisture at the wilting point, and,  $s^*$  is the soil moisture at the stress point.

Having solved for the components of Equation 3, we can use Equations 4 and 7 express  $ET(s)$  as follows:

$$ET(s) = \begin{cases} 0 & 0 \leq s < s_h \\ \left(\frac{s - s_h}{1 - s_h}\right)^{q_e} ET_{max} e^{-0.5 \cdot LAI} & s_h \leq s < s_w \\ \left(\frac{s - s_h}{1 - s_h}\right)^{q_e} ET_{max} e^{-0.5 \cdot LAI} + \frac{s - s_w}{s^* - s_w} K_c T_{max} & s_w \leq s < s^* \\ \left(\frac{s - s_h}{1 - s_h}\right)^{q_e} ET_{max} e^{-0.5 \cdot LAI} + K_c T_{max} & s^* \leq s \leq 1 \end{cases} \quad (8)$$

Figure 4 shows the functional form of evaporation and transpiration as a function of relative soil moisture content for a clay loam soil in which  $s_h$  is 0.42,  $s_w$  is 0.53, and  $s^*$  is 0.78.

### 2.2.1.4. Leakage

Whenever daily soil moisture exceeds the soil field capacity,  $s_{fc}$ , we calculate leakage of water out of the plant root zone. The instantaneous rate of leakage is determined by the hydraulic conductivity,  $K(s)$  [mm/day], which is given by

$$L(s) = K(s) = \frac{K_s}{e^{\beta(1-s_{fc})} - 1} (e^{\beta(s-s_{fc})} - 1), \quad (9)$$

where  $K_s$  is the saturated hydraulic conductivity [mm/day] and  $\beta$  is a soil-specific parameter that governs the shape of the relationship between saturation and hydraulic conductivity; that is,  $\beta = 2b + 4$ , where  $b$  is a coefficient governing the power-law form of the soil-water retention curve (Laio et al., 2001).

$$\Psi_s = \bar{\Psi}_s s^{-b} \quad (10)$$

where  $\Psi_s$  is the soil matrix potential at a given value of soil moisture and  $\bar{\Psi}_s$  is a representative value of soil matrix potential at saturation (i.e., water potential at air-entry) for specific soil types. Values of  $b$  and  $\bar{\Psi}_s$  are based on soil texture and are taken from the empirically determined coefficients presented in Clapp and Hornberger (1978).

Following an input of rainfall such that  $s_0 > s_{fc}$ , Equation 1 becomes an expression of soil moisture decay. In the absence of evaporative losses, we can simplify leakage to

$$L(s) = -nZ_r \frac{ds}{dt} \quad (11)$$

Then we use Equations 9 and 11 to solve for the initial condition,  $s_0$ , which yields the analytical solution for total daily leakage when  $s > s_{fc}$ :

$$L = \frac{nZ_r}{\beta} \ln \left[ e^{\beta(s_0 - s_{fc})} - e^{-m\beta} (e^{\beta(s_0 - s_{fc})} - 1) \right] \quad (12)$$

where

$$m = \frac{K_s}{nZ_r (e^{\beta(1-s_{fc})} - 1)} \quad (13)$$

### 2.2.1.5. Runoff

Our model only considers saturation excess overland flow, so that when the balance of daily rainfall, evaporation, and leakage leads to an excess of soil saturation, the excess is converted to surface runoff. Thus, we can write

$$Q(s) = \begin{cases} 0 & 0 \leq s \leq 1 \\ (s-1)nZ_r & s > 1 \end{cases} \quad (14)$$

### 2.2.2. Plant Water Stress

Water stress during the growing season affects the physiology of plants and is crucial in determining the success of a crop. Soil moisture excursions below the wilting point,  $s_w$ , and the point at which transpiration is reduced,  $s^*$ , can lead to reduced biomass production and eventual crop failure. By defining the duration and frequency of soil moisture deficits probabilistically, we gain insight into the yield reductions from intense water stress such as drought and the likelihood of crop failure. The mathematical derivations for these dynamics are described in previous work (e.g., Rodríguez-Iturbe & Porporato, 2007).

First we calculate static water stress: a measure of the mean vegetation water stress incurred during a given excursion below  $s^*$  (Porporato et al., 2001).

$$\zeta(t) = \left[ \frac{s^* - s(t)}{s^* - s_w} \right]^{q_{\text{stress}}}, \quad \text{for } s_w \leq s(t) \leq s^* \quad (15)$$

where  $\zeta(t)$  is the static water stress or instantaneous water stress as it is the measure of stress at one point in time and  $q_{\text{stress}}$  represents the crop's sensitivity to the magnitude of excursions below the stress point.

Although the static stress describes the mean water deficit relative to  $s^*$  and  $s_w$ , we are also interested in the duration and frequency of water deficit. Following the work of Rodríguez-Iturbe and Porporato (2007, p. 67), we also define two other random variables: the average length of time in days in which soil moisture is below the threshold,  $T_\zeta$ , and the number of times the threshold is crossed during a season,  $n_\zeta$ . Next, we calculate dynamic water stress,  $\theta$ , a measure of the crop's total water stress during the growing season that characterizes the duration and frequency of exposure to water stress:



$$\theta = \begin{cases} \left( \frac{\bar{\zeta} \bar{T}_{s^*}}{kLGP} \right)^{n_s^{-r}} & , \bar{\zeta} \bar{T}_{s^*} < kLGP \\ 1 & , \bar{\zeta} \bar{T}_{s^*} \geq kLGP \end{cases} \quad (16)$$

where  $\bar{\zeta}$  is the average static water stress incurred over the growing season;  $\bar{T}_{s^*}$  is the average duration of excursion;  $n_s$  is the number of occurrences of these excursions during the growing season;  $LGP$  is the length of the growing period in days;  $k$  is the portion of the season that stress can occur before the crop fails; and  $r$  is a normalization parameter for the number of excursion below the stress point. We use the values for  $r$  and  $k$  noted in Table 3. The  $r$  parameter is defined as in Porporato et al. (2001), and the  $k$  parameter is selected in order to approximate a characteristic rainfall yield relationship such as in Guan et al. (2017). Lastly, we calculate seasonal crop yields,  $Y$ , as a function of dynamic water stress:

$$Y = Y_{max}(1 - \theta) \quad (17)$$

where the maximum yield per unit area (hectare) is  $Y_{max}$ . This value of  $Y_{max}$  is specific to the  $LGP$  of the crop as estimated by the linear regression in Figure 3. The maximum potential yield for a variety with a 180 day  $LGP$  is 4.26 metric tons per hectare. We conducted a sensitivity analysis to test different values of  $r$ ,  $k$ ,  $q_{stress}$  and  $q_e$  on yields in Figure B1 and discuss the need for improved measurements of intra-seasonal crop stress in Appendix B.

### 2.3. Model Implementation

In order to conserve the water balance, we implement the model piecewise. First, we calculate saturation excess,  $Q(t)$ , which is caused by an input of rainfall that leads to the soil moisture being above saturation (i.e.,  $s > 1$ ). Therefore, any rainfall that causes  $s$  to be greater than 1 is instantaneously routed as runoff, and thus there is an explicit upper bound of  $s$  which is 1 as shown in Equation 8. We then calculate both leakage and evapotranspiration using the same  $s$  value and within the same time step. Lastly, once we have values of  $L(t)$  and  $ET(t)$ , we update the water balance and the soil moisture.

We run the model for 10,000 simulations using the following initial conditions and parameters. We use the Ol Jogi Farm rainfall climatology (10-day rainfall parameters estimated from daily rainfall records between 1967 and 1998), a clay loam soil texture, and 180-day maize variety, which are typical values for the study site. We selected a planting date of March 1 (Julian day 60) for model calibration and simulations. Farmers vary in their planting practice but generally plant at the start of the long rains after  $\sim 20$  mm of rainfall has fallen. We selected March 1 because it was the most frequently planted week for the long rains among surveyed farmers in our study site. To determine the initial condition for our simulations, we first run the model for 60 days ( $T_{burn}$ ) before the planting date and run 1,000 simulations ( $N_{burn\_sim}$ ) to get an average value of  $s$  for the first day of the season. Then we use this average value as the initial condition for each of our subsequent simulations of the growing season.

#### 2.3.1. Impacts of Maize Variety on Farming Outcomes

We continue with the model parameters previously described to compare yield outcomes for different maize varieties (e.g., Ol Jogi rainfall climatology, clay loam soil, planting day 60 etc.). We run the simulations for three categories of varieties: early, medium, and late maturing. The simulations have the same precipitation forcing for all the varieties, and the only lever that is being changed for this experiment is the length of the growing period ( $LGP$ ). The maize varieties have different times to maturity that vary in five-day increments between 80 and 180 days: early maturing between 80 and 110 days, medium maturing between 115 and 145 days, and late maturing between 150 and 180 days (all inclusive). We designate 21 different maize varieties to represent all of the five-day increments between 80 and 180 days. These 21 varieties are each simulated 500 times, resulting in 10,500 total simulations.

#### 2.3.2. Impacts of Rainfall Climatologies on Farming Outcomes

We use two rainfall gauges to determine the 10-day average rain depth per event ( $\alpha$ ) and rain event frequency ( $\lambda$ ) used as model parameters, which are described in Table 2. First, we use the long-term average

Ol Jogi Farm rainfall climatology for running the model as this location is climatologically representative of semiarid small-scale producers in the region who depend on rainfall. We use this station for the model simulation results in Section 3.1 through Section 3.3.

We use the longest station gauge record (79 years), Jacobson Farm rainfall climatology, to analyze long-term temporal changes in crop production and crop failure in Section 3.5. We define three eras of crop production: two extreme conditions (1930s rainfall climatology and 2010s rainfall climatology) and the average rainfall conditions. We extract 10-day rain depth per event ( $\alpha$ ) and rain event frequency ( $\lambda$ ) values as follows. To represent average annual change in either parameter, we use the average 10-day  $\alpha$  and  $\lambda$  values, which considers the entire rainfall record and corresponds to the climate in the middle of the record. We adjust the long-term average values for each 10-day increment in order to obtain historical (1930s) or present (2010s) values of the parameters 10-day increment. To estimate the past, “1930s,” 10-day rain depth per event ( $\alpha$ ) and rain event frequency ( $\lambda$ ) values we simply apply the trend line to each of the individual average 10-day increment.

We recognize that extrapolating trends in rainfall from historical observations may depend on the period and length of observation (as shown in Figure 2). For our analysis, we wanted to represent how rainfall conditions, specifically shifts in intensity and frequency, have changed within several generations of farmers, that is from the 1930s to 2010s. For example, we calculate the 10-day rain depth per event ( $\alpha$ ) for the 1930s climatology by taking the average 10-day alpha and subtracting it by the slope of the trend line multiplied by 40 years. For the present “2010s” values we add the slope of the trend line multiplied by 40 years. We then use these three sets of average rain depth per event ( $\alpha$ ) and rain event frequency ( $\lambda$ ) values to run the simulations for the three subsetted periods. We run 100,000 simulations for each period with the parameters used in Table 3. Therefore, the only source of variability in this counterfactual analysis of crop failure and yields is the rainfall generator.

### 3. Results

#### 3.1. Time-Varying Impacts of Seasonal Water Availability Using the Ol Jogi Rainfall Climatology

Figure 5 (bottom panel) shows the average soil moisture content for 10,000 growing seasons of a 180 day variety planted on day 60 (approx. March 1) using the Ol Jogi rainfall climatology. The 10-day rain depth per event ( $\alpha$ ) and rain event frequency ( $\lambda$ ) parameters used to generate rainfall are variable over the 6 month period. The rain event frequency,  $\lambda$ , increases more than three-fold during the first 80 days of the season while the average depth per storm,  $\alpha$ , stays relatively constant throughout the 180 day growing season with values between 8 and 13 mm of rain (Figure 5, top). On dekads 15 and 16 (~80–90 days into the growing season), the rain event frequency,  $\lambda$ , drops and levels off indicating the cessation of the long rains season. During this period of rainfall variability, the crop coefficient follows a step-wise function in which water requirements are low before steadily increasing when the crop begins to develop (Figure 5, middle plot).

For the first 80 days of crop growth, the soil moisture levels increase steadily. At approximately day 80, the crop coefficient peaks at a value of 1.2, which is subsequently met with a decline in the soil water content (Figure 5, bottom). During this stage of peak water requirements from day 80 to 140, the crop enters its reproductive stage in which flowering and grain-filling occur. Concurrently, the water availability decreases as  $\lambda$  values decline near the end of the long rains and the relative soil moisture,  $s$  decreases from ca. 0.7 to 0.6. At the end of the growing season, the soil moisture levels slowly decline and flatten until day 180 when the crop coefficient linearly decrease to a final value of 0.6. Interestingly, the crop coefficient and  $s$  align reasonably well over the course of the season. This alignment indicates that the  $K_c$  function that we use, which is derived from regional studies conducted by the FAO and previously described in Section 2.2.1.3, works reasonably well for our study location as shown for a late maturing 180-day variety.

We then investigate the impact of stochastic rainfall on soil water availability for a single season. Figure 6a shows an example time series of simulated daily rainfall for a late maturing 180-day variety planted on day 60 using the Ol Jogi Farm rainfall climatology. As we expect, soil saturation increases in the early to middle part of the season (around days 50 to 100 in Figure 6b), which aligns with the peak of the rainfall season Figure 6a. The crop is moderately stressed over the entire season because the majority of the soil saturation

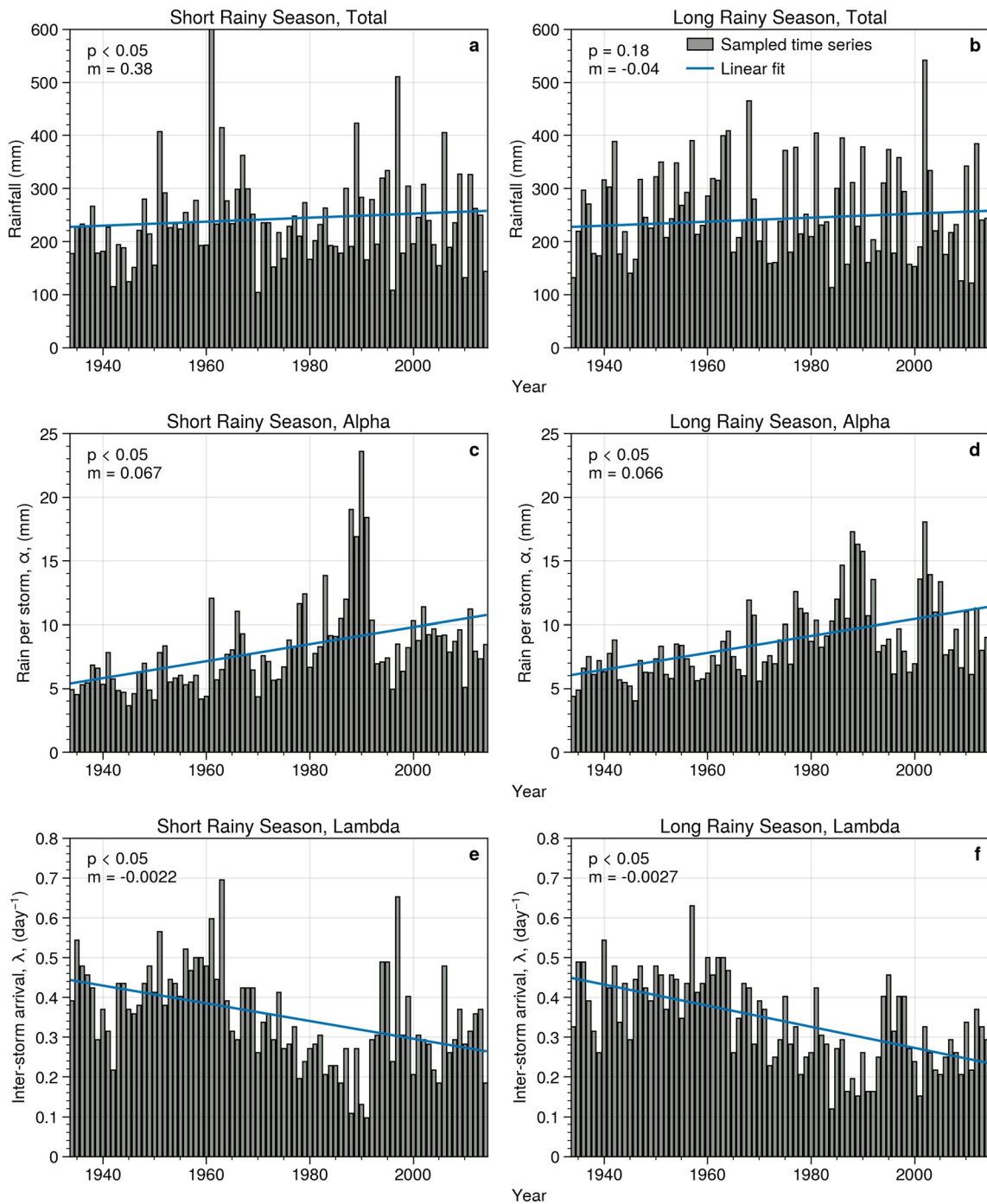


**Figure 2.** Time series for the Jacobson Farm station which has a 79-year record length. Significant trends ( $p < 0.05$ ) are shown in plots (a, c, d, e, f) per the modified Mann-Kendall test.

time series falls between the stress and wilting points. In this particular simulation, the crop experiences the lowest levels of stress between days 60 to 80 whereas the highest levels of stress occur for the first 40 days of the growing season and between days 130 and the end of the growing season.

For the simulated 10,000 growing seasons, we investigate the distributions and time series of average soil saturation and static stress in Figure 7. We find a seasonality in water availability in which soil moisture peaks between days (day of year) 135 and 145 for all simulations. The average soil moisture begins to

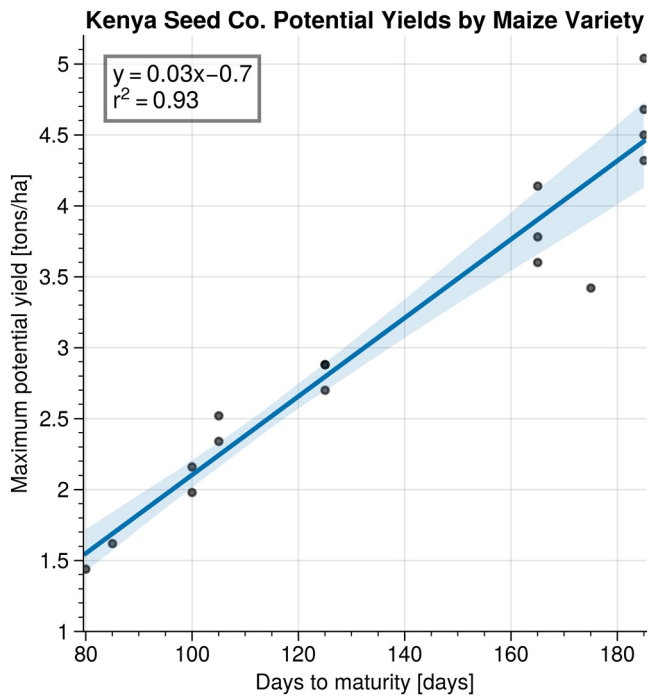


**Figure 3.** Linear regression with 95% confidence interval. Data are maize varieties sold by Kenya Seed Company. We removed two varieties from the data set (PH1 and PH4) because the days to maturity information from Kenya Seed contradicted what is known about these four-month varieties. Data retrieved August 19, 2019 from <https://web.archive.org/web/20190216031348/http://kenyaseed.com/gallery/maize/>.

decrease around day 145 before stabilizing around day 170. The simulations are prone to water deficit during the earliest and latest parts of the season in which the average saturation starts at 0.5 and ends the season around 0.55, on average. The crop is at the highest points of average static stress during these periods as shown in Figure 7d.

The crop is generally stressed over the course of the season because the stress point is 0.78 and the saturation time series in Figure 6b falls below and around the stress point for the majority of the season. The stress values of the crop ranges between 0 and 1, and in the time series, we see a larger increase in stress compared to the relative saturation time series. Additionally, we see greater variability in stress values compared to saturation values as the confidence intervals for stress are very wide especially in the later part of the season. This is due to the nonlinearity introduced in the conversion from relative saturation to stress.

### 3.2. Dynamic Water Stress

To convert average static stress into a yield metric that allows for the probability of crop failure, we use the dynamic stress equation. Dynamic water stress considers both the frequency and duration of excursions below the stress point and is used to estimate end-of-season yield as a fraction of the maximum possible yield for that variety as shown in Equation 17. Calculating yield in this way is typical in the literature on numerical simulations of climate variability and crop yields (Roche et al., 2020; Van Ittersum et al., 2013). We show the PDF of dynamic water stress in Figure C1.

As shown in Figure 8 for the 180-day variety, the relationship between rainfall and yield is not a linear one, but rather is asymptotic. We also include the relationships between seasonal rainfall and yield for the early,

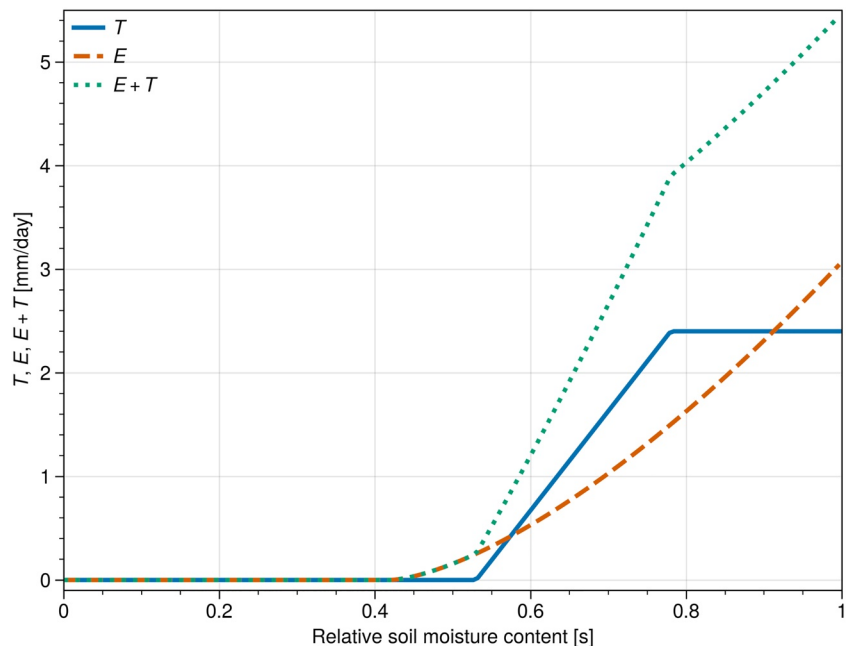


**Figure 4.** Evaporation, transpiration, and evapotranspiration as functions of relative soil moisture where Leaf Area Index is 1.5 and  $s_h$  is 0.42. Other climate and crop parameters are those listed in Table 3.

**Table 2**  
*Characteristics of Rain Gauges Used in Model Simulations<sup>a</sup>*

Site	Latitude	Longitude	Mean annual rainfall, mm	Altitude, m.a.s.l.	Start year	End year
Jacobson Farm	0.04	37.04	735	1,875	1934	2014
Ol Jogi Farm	0.31	36.94	538	1,741	1967	1999

<sup>a</sup>Start and end years are the years when the rainfall records began and ended for each rain gauge.

medium, and late maturing varieties categories in Appendix D. As the crop experiences more rainfall, yields increase up to a ceiling which is defined by the yield potential of the cultivar. We find that yields are closer to the maximum potential yield with seasonal rainfall totals greater than ca. 600 mm. When the seasonal rainfall totals are less than ~450 mm, the possibility of crop failure is introduced. We find that seasonal rainfall totals between ca. 200 and 450 mm, there is a large range in possible outcomes for farmers. For a given seasonal total within this range, we find that farmers can reach up to 60–75 percent of the maximum possible yields while others experience total crop failure. This relationship also holds true for early and medium maturing varieties as shown in Appendix D. For seasonal rainfall totals below 200 mm or so, the majority of simulations result in total crop failure. Therefore while the seasonal total of rainfall is important, there are also characteristics of within season rainfall that have a pronounced effect on yield outcomes.

### 3.3. Cultivar Choice Mediates Probability of Crop Failure

We then investigate the effect of cultivar choice (i.e., *LGP*) on yield and crop failure using the methods described in Section 2.3.1. Figure 9 shows the joint probability distribution of yield and rainfall for three categories of maize varieties: early, medium, and late maturing. The average rainfall and yield for each category of maize varieties is denoted as a black “x.” In Table 5, we provide the average statistics that correspond with Figure 9. We find that the average seasonal rainfall increases in proportion to the length of the growing season for each of the maize varieties categories. Because early maturing varieties require less time to grow (e.g., 80–110 days) compared to late maturing varieties (e.g., 150–180 days), they receive less average seasonal rainfall.

Despite having lower seasonal totals due to their shorter maturity period, early maturing crops are more likely reach their maximum potential yields while medium and later maturing crops only gain a fraction of their maximum yields (Appendix D). Additionally, under low seasonal rainfall totals, medium- and-late maturing crops have a higher incidence of crop failure, which is indicated by the spread of probability densities around 0 yield between 0 and 300 mm of rainfall in Figure 9. In comparison, early maturing crops are less likely to fail, which is indicated by the less dense probabilities below 200 mm of rainfall. These trends are reflected in the percentage of simulations that resulted in crop failure: approximately 27%, 32%, and 35% for early maturing, medium-maturing, and late-maturing, respectively, as shown in Table 5. Late-maturing varieties also have a larger spread in potential yields compared to early- and medium-maturing varieties.

### 3.4. Regional Rainfall Climatology Trends

We investigated interannual trends in seasonal totals, storm depth and inter-storm arrival rate for the two rainy seasons. Overall, we find that changes in seasonal totals are minimal across the stations, shown in Table 4, and as visualized for Jacobson Farm in Figure 2. However, we do find significant trends for increasing intensity,  $\alpha$ , and decreasing frequency,  $\lambda$  in both rainfall seasons ( $p < 0.05$ , Table 4) using the modified Mann-Kendall statistical test. Comparatively, total rainfall for both seasons and annual rainfall shows a muted change with fewer stations showing significant trends. Our results are consistent with those of Franz et al. (2010), which analyzed a less recent data set of 11 stations in the same region. In Figure 2, we use the Jacobson Farm rain gauge which has the longest record (79 years) to show the shifts in rainfall processes that occur in this region. Here, we see that while total rainfall for either season does not change significantly, we see an increase in  $\alpha$  and decrease in  $\lambda$  over the period ( $p < 0.05$ , Figure 2). This indicates that storms are becoming more intense and less frequent. The relevance of this interannual variability in rainfall is further discussed in Section 4.

**Table 3**  
*Model Parameters and Their Sources*

Type	Parameter	Value
Climate parameters	$LGP$	180 days
Crop parameters	$I_e$	1 mm LAI <sup>-1</sup>
	$Z_r$	400 mm <sup>a</sup>
	$T_{max}$	4.0 mm day <sup>-1</sup>
	$ET_{max}$	6.5 mm day <sup>-1b</sup>
	$K_{c,max}$	1.2 (dim) <sup>c</sup>
	$LAI_c$	3.0 mm <sup>2</sup> mm <sup>-2d</sup>
	$q_e$	1.5 (dim)
	$q_{stress}$	2 (dim)
	$p$	1 (dim)
Soil parameters (clay loam)	$k$	0.25 (dim)
	$Y_{max}$	4.26 t ha <sup>-1</sup>
	$s_w$	0.53 (dim) <sup>f</sup>
	$s^*$	0.78 (dim) <sup>f</sup>
Simulation parameters	$N_{sim}$	10,000 seasons
	$N_{burn_{sim}}$	1,000 seasons
	$T_{burn}$	60 days

<sup>a</sup>Nyakudya and Stroosnijder (2014). <sup>b</sup>Barron et al. (2003). <sup>c</sup>Allen et al. (1998). <sup>d</sup>C. A. Williams and Albertson (2004). <sup>e</sup>Porporato et al. (2001). <sup>f</sup>Clapp and Hornberger (1978).

### 3.5. Long-Term Trends in Yield and Crop Failure Using the Jacobson Farm Rainfall Climatology

After changing 10-day average rain depth per event ( $\alpha$ ) and rain event frequency ( $\lambda$ ) values to represent those in an earlier era (1930s) and present day (2010s) at Jacobson Farm, we show how cropping outcomes have changed over the 80 year record in Figure 10 and Table 6. During this period, we see the rain depth per event ( $\alpha$ ) and rain event frequency ( $\lambda$ ) change where the average  $\alpha$  values increased from 5.71 mm per storm event in the 1930s to 10.99 mm per storm event in the 2010s. Conversely, the average  $\lambda$  values decreased from 0.35 rainfall events per day in the 1930s to 0.16 rainfall events per day in the 2010s. We see a marked shift in the average seasonal rainfall generated from the simulations, which exhibits an inverted U-shape. There is an increase in average rainfall between the 1930s and the middle of the record from 362 mm (standard deviation, SD, 139 mm) to 385 mm (SD 154 mm), and a decrease to the later part of the record in the 2010s of 316 mm (SD 136 mm). The average seasonal rainfall total in the latest part of the record was dramatically lower than the earlier two data points.

Interestingly, average crop yields also follow the inverted-U shape: At the start of the record, average crop yields were the lowest at 0.72 t/ha. Crop yields increased to the maximum of these three eras in the middle of the record to 1.05 t/ha and then decreased again to 0.84 t/ha in the 2010s. Crop failure rates show a similar pattern in which the crop failure rate was lowest in the middle part of the record (31%) and highest during the early part of the record (48%) and the present day crop failure rate is in between at 33%. The coefficient of variation of rainfall increased from 0.38 in the 1930s to 0.43 in the 2010s.

## 4. Discussion

### 4.1. Rainfall Trends and Impacts on Maize Production

Warming global temperatures directly cause interannual variability in rainfall—that is, the shift towards fewer and more intense storms (IPCC, 2007)—as observed at Jacobson Farm and other gauges in the field

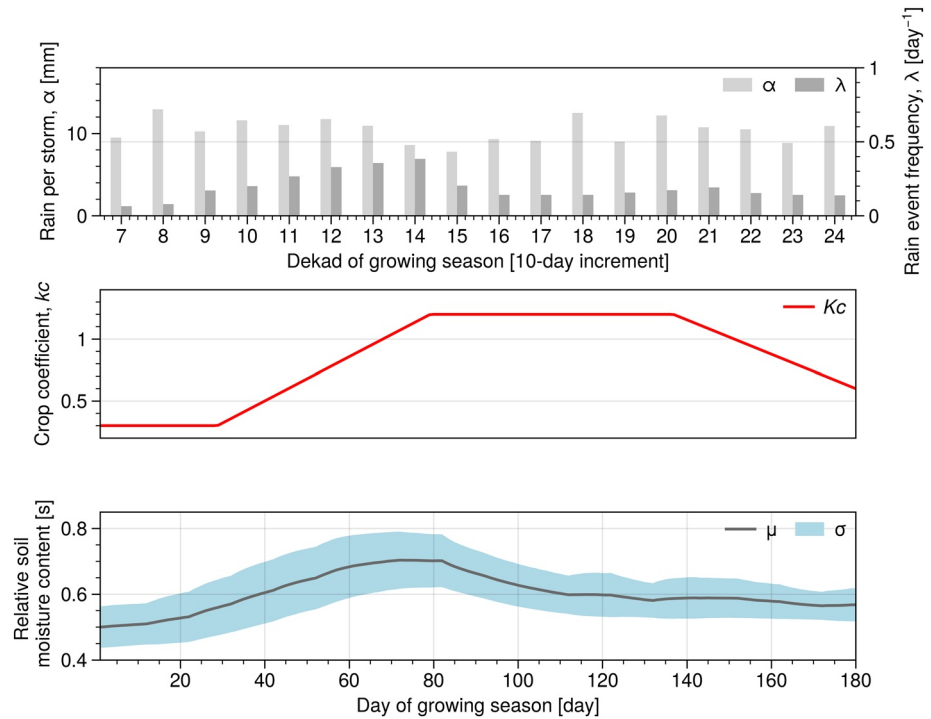


**Figure 5.** Three time-varying model parameters: 10-day average rain depth per event ( $\alpha$ ) and rain event frequency ( $\lambda$ ) values starting with the planting date (March 2–11 in non-leap year) (top); daily crop coefficient (middle); and daily saturation (bottom).

site (Table 4). With air temperatures and atmospheric water vapor rising in East Africa as well as globally, extreme precipitation events are expected to increase (Christensen et al., 2007; Trenberth, 2011). We find that while rainfall seasonal totals are not changing, the average rainfall event depth and frequency have changed in several sites in Laikipia, Meru and Nyeri counties.

When considering the extremes of the 80-year rainfall record (i.e., 1930s vs. 2010s rainfall climatology), we see changes in cropping outcomes among maize farmers. Overall, we find an inverted-U shaped relationship from the three time periods of interest where the average yields peaked and the probability of crop failure was lowest in the middle of the time series. We found that the average seasonal rainfall shifted from a period of high seasonal rainfall in the 1970s and lower seasonal rainfall in the 2010s. Our results indicate

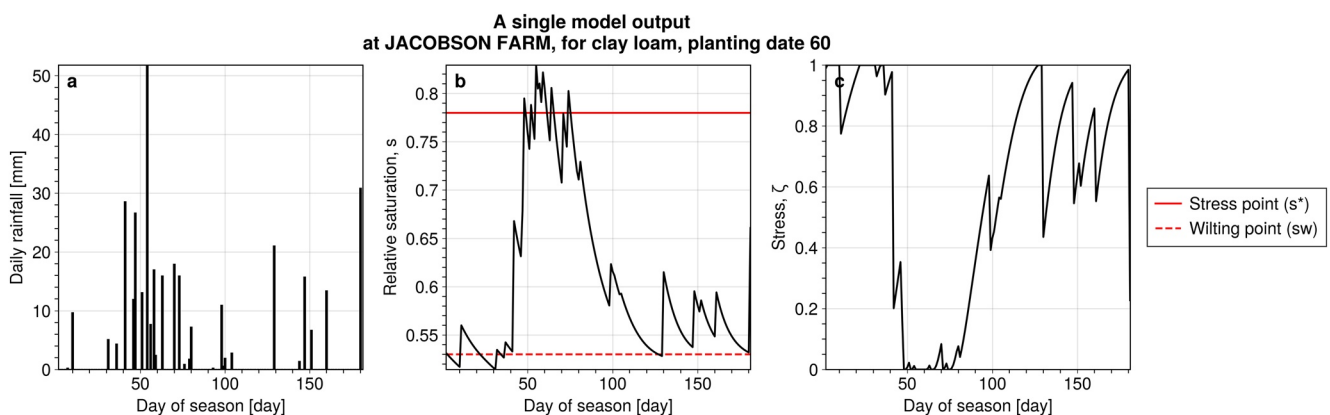


**Figure 6.** Time series of (a) precipitation, (b) relative saturation, and (c) static stress for a single simulation. Rainfall climatology is determined by Ol Jogi Farm station data, soil texture is clay loam, maize variety is 180 days, and planting date is day of year 60. Soil wilting point is red dashed line. Stress point (the point at which transpiration starts being reduced) is the solid red line. For a clay loam soil the stress point in units of saturation is 0.78 and the wilting point is 0.53.

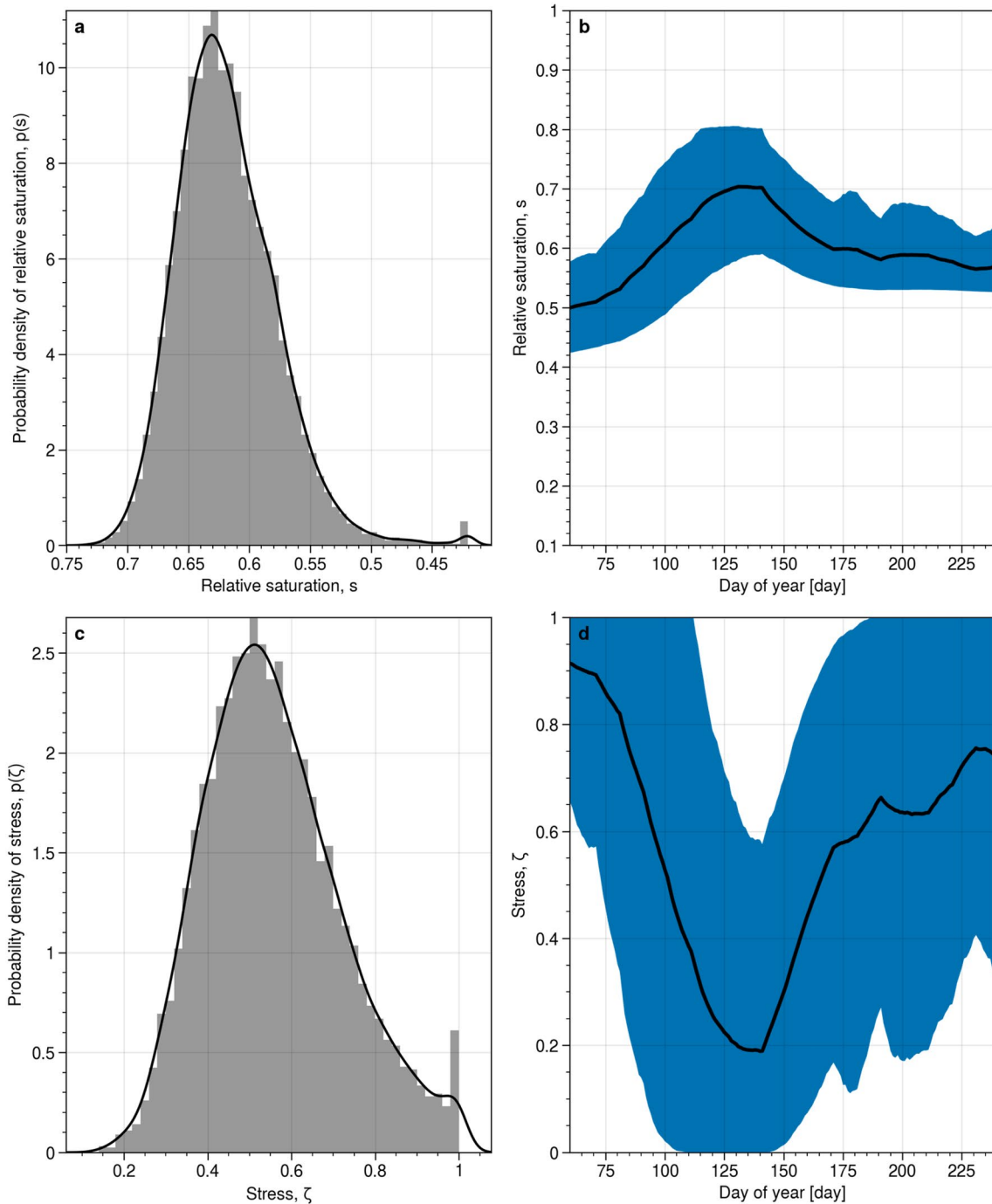


**Figure 7.** Probability distribution functions and time series of average soil saturation and stress with 90 and 10% confidence intervals for 10,000 simulations. Model parameters used are the same as those in Figure 6.

that the environmental conditions for growing maize were most difficult in the earlier part of the record, they became easier in the 1970s, and now are becoming more difficult again. The reasons for these changes stem from the interactions between shifts in mean seasonal rainfall, increasing storm depths, and decreasing storm even frequency. It is notable that despite the very low seasonal rainfall totals in the 2010s, the average yield is not lowest and the crop failure rate is not the highest seen across the three eras. The nonlinear relationships between crop yields and both seasonal rainfall totals and rainfall statistics (average depth and frequency) make it difficult to predict yields using a single rainfall metric. Previous work has demonstrated



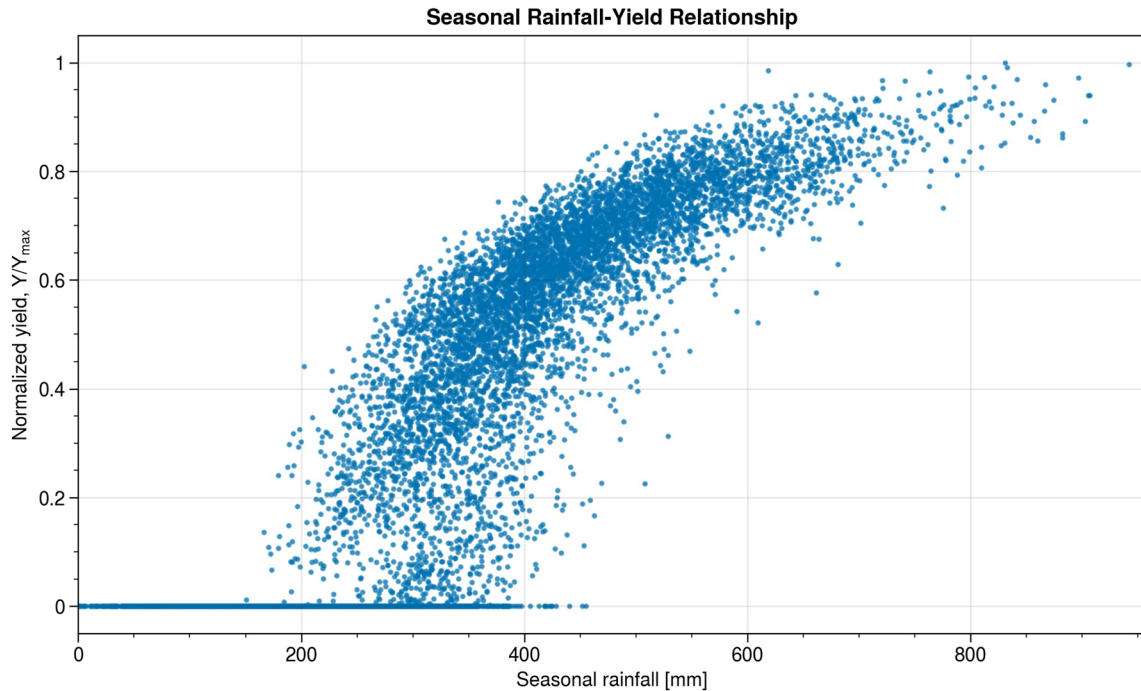


**Figure 8.** Scatterplot of seasonal rainfall and yield for 180-day maize and study site conditions. End of season yields are normalized by the maximum yield for all 10,000 simulations: 2.8 t/ha.

similar findings such that the intensity and duration of individual rainfall events is important for hydrological partitioning of precipitation in addition to annual or seasonal totals (Apurv et al., 2017; Kipkemoi et al., 2021; Singer & Michaelides, 2017; Taylor et al., 2013). We also find an increase in the coefficient of variation in rainfall showing that farmers experience increasingly variable rainfall conditions.

Previous studies have sparked concern over the future of rainfall in East Africa and formed a consensus about the role of climate change in influencing rainfall patterns (Nicholson, 2017; Shongwe et al., 2011). Specifically, these studies have demonstrated negative trends in the magnitude of the long rains (March–May) in East Africa and the Horn of Africa Drylands (Funk et al., 2019; Funk, Harrison, et al., 2018; Liebmann et al., 2014; Lyon & DeWitt, 2012; A. P. Williams & Funk, 2011). Other studies have shown regional trends towards more extreme rainfall events (Harrison et al., 2019), particularly for the short rains

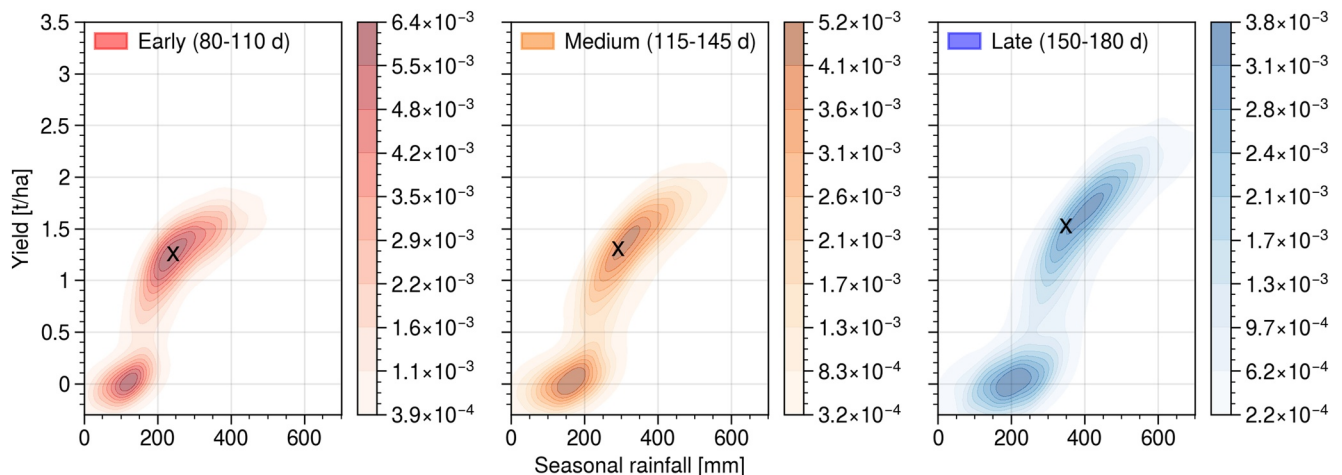


**Figure 9.** Joint probability distribution of three maize varieties categories using Ol Jogi rainfall climatology. The average rainfall and yield for each subplot is denoted with “x.” Non-zero values of yield were used to calculate this average.

**Table 4**

Summary of Rainfall Statistics With Gauge Record Lengths Greater Than 40 Years ( $n = 39$ ) for Short Rains (SR, March Through May), Long Rains (LR, October Through December) or Both Seasons

Parameter description	Season	Percent of stations with significant trends ( $p < 0.05$ )	Mean slope of all stations (Sen's method)	Standard error of slopes
Total rainfall [mm]	SR	8.75	0.2863	0.4469
Total rainfall [mm]	LR	1.25	-1.115	0.5240
Annual rainfall [mm]	Both	12.82	-0.0673	0.6194
Average depth per event $\alpha$ [mm]	SR	20.00	0.0654	0.0153
Average depth per event $\alpha$ [mm]	LR	21.25	0.0641	0.0180
Average event frequency $\lambda$ [ $\text{day}^{-1}$ ]	SR	33.75	-0.0010	0.0006
Average event frequency $\lambda$ [ $\text{day}^{-1}$ ]	LR	32.50	-0.0030	0.0005

Note. We computed a modified Mann-Kendall test to designate significant trends ( $p < 0.05$ ). Data source: CETRAD.

(October–December) (Shongwe et al., 2011) and in central Kenya (Schmocker et al., 2016). In addition to decreased seasonal totals, trends towards more extreme rainfall events will likely contribute to decreased end of season yields and increased rates of crop failure due to the timing and nature of rainfall and crop water requirements of maize over the season. Increasingly heavy rainfall events pose a threat to crop production due to extreme surface runoff and subsequent erosion or from flood events (Liniger & Thomas, 1998; Liniger & Weingartner, 1998).

Small-scale producers depend on reliable rainfall. We show that maize yields are lower in the present day in comparison to yields 40 years ago due to reduced seasonal rainfall totals and increased rainfall variability. In order to attain end of season yields that are profitable, maize growers must avoid both sodden conditions due to extreme rainfall and drought conditions caused by dry spells (Rigden et al., 2020). Our results show that despite having seasonal rainfall totals that should be adequate for maize growth, the end of season yields and chance of crop failure are highly variable. This is because the crop coefficient of maize does not necessarily align with the periods of highest rainfall when planting is conducted in early March and in these systems where irrigation may be absent. For this reason, hybrid maize has been developed to withstand variable rainfall and drought during the growing season. We also find that intraseasonal rainfall variability has a pronounced impact on farmer outcomes for varieties with different maturity periods.

#### 4.2. Cultivar Choice Moderates Exposure to Stress

Varieties with shorter maturation periods reduce their exposure to water stress and fail less often compared to varieties with longer maturation periods. We show that modest decreases in relative soil saturation lead to dramatic increases in the water stress of simulated maize. When the length of the growing period is shortened for an early maturing crop to reach the flowering and grain-filling phenological stages faster, there is a reduced chance of exposure to water deficits. Therefore, we find that early maturing varieties have a shorter exposure to rainfall variability and therefore are less likely to fail whereas long-maturing varieties grow for

**Table 5**

Summary Statistics for Three Maize Variety Categories

Statistic	Early (80–110 d)	Medium (115–145 d)	Late (150–180 d)
Average seasonal rainfall (mm)	221.6	270.8	328.1
Average yield (t/ha)	1.18	1.23	1.45
SD yield	0.36	0.46	0.55
Crop failure (%)	26.8	32.0	34.9

Note. These results are from the methodology described in Section 2.3.1 and explained in Section 3.3. Average seasonal rainfall is increasing in proportion to the length of the growing period (LGP) in which early maturing varieties take between 80 and 110 days to grow; medium maturing take 115–145 days; and late maturing 150–180 days. SD, standard deviation.

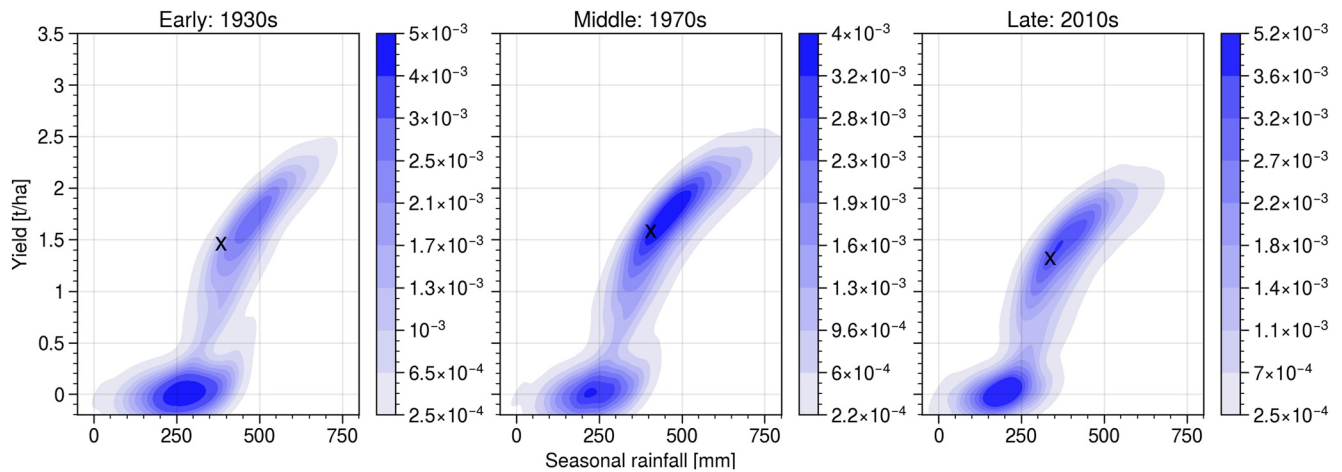


**Figure 10.** Historical change in seasonal rainfall and yields for Jacobson Farm climatology. We defined three eras of rainfall conditions in which we set the rain depth per event ( $\alpha$ ) and rain event frequency ( $\lambda$ ) parameters based on the relative trend line in Figure 2. The average rainfall and yield for each subplot is denoted with “x.” Non-zero values of yield were used to calculate this average.

longer periods and are more susceptible to longer periods with no rainfall. These early maturing varieties escape longer dry periods and therefore may be a better option for small-scale maize producers under increased levels of rainfall variability.

Cultivar choice is one of the primary adaptation strategies that farmers can control to minimize the stress experienced by the crop. We show that early maturing crops are the best choice given their fast maturity period and lowest probability of crop failure. Late maturing crops will produce higher yields in the simulations that do not fail, however, they are exposed to longer periods of no rainfall due to taking more time to grow and therefore have a higher risk of crop failure. Early maturing varieties are the least likely to fail just on the basis of requiring less time to grow and thus have a shorter exposure to the rainfall process. Furthermore, early maturing varieties are often bred or have been genetically modified to be drought tolerant. Drought tolerance is often developed for a specific set of environmental conditions and thus can be hyper-localized.

In a survey of 500 East African farming households, Erenstein et al. (2011) found that the most desired attribute of maize varieties was yield potential followed by early maturity. These characteristics were perceived to be more important than drought tolerance. Maize cultivars can exhibit one of two traits: drought avoidance as in the case of early maturing varieties and drought tolerance in the case of hybrids that are bred to tolerate reduced available water. Early maturing varieties are considered drought avoidant because they are thought to complete their most drought-sensitive stage (flowering) before a drought occurs such as at the ending of a growing season (Barron et al., 2003; Morris, 2001).

**Table 6**  
Summary Statistics for Historical Trends in Crop Failure and Yield

Metric	Early: 1930s	Avg: 1970s	Late: 2010s
Average seasonal rain depth ( $\alpha$ ) (mm)	5.71	8.33	10.99
Average seasonal rain frequency ( $\lambda$ ) ( $\text{day}^{-1}$ )	0.35	0.26	0.16
Average seasonal rainfall (mm)	362.3	384.6	316.1
SD rainfall	139.2	154.3	136.0
CV rainfall	0.38	0.40	0.43
Average yield (t/ha)	0.72	1.05	0.84
Probability of crop failure (%)	48.3	30.9	32.8

*Note.* Parameters set to Jacobson Farm with a planting date of day 60 and a 180 day maize variety. SD, standard deviation. CV, coefficient of variation.

We show that by growing a late maturing variety, the crop is still subject to terminal drought and crop failure due to the timing of rainfall throughout the season. However, a trade-off exists in selecting a late maturing variety. As shown in the empirical data of maize cultivars and yield (Figure 3), there is an opportunity for higher yields for late maturing maize varieties. In cases where farmers do not have access to irrigation and would prefer a crop that has a greater chance of success despite a potential yield penalty, farmers may prefer early maturing crops (Barron et al., 2003).

There are two possibilities that plant breeders and farmers can elect for: to optimize for survival by minimizing the variance of stress experienced by the crop or to optimize for greater biomass in order to get the maximum yield. In light of this, farmers may be interested in maximizing their yield as well as limiting crop failure by planting a medium maturing variety. However, in areas with high rainfall variability there might be reason to plant only early maturing varieties either with the intent of minimizing crop failure or in order to double crop within the season. In these settings where a farmer's goal is to prevent crop failure, early and extra early maturing varieties are more effective for a planting date of March 1 as described in our model. There may be a role for varieties with other maturity durations when using different planting dates.

#### 4.3. Declining Yields, Increasing Crop Failure Rates and Household-Level Impacts

The increased variability in rainfall and decreased seasonal totals have serious implications for agriculture in East Africa and other regions of the African continent where large portions of the population suffer from food insecurity (Funk & Brown, 2009). These changes in mean annual rainfall and increased storm size may make it increasingly difficult for farmers to practice agriculture as they have done so in the past. As shown in the temporal analysis of rainfall trends, the timing and distribution of rainfall has changed within one to two generations of farmers.

Climate change and climate variability impacts can shock the economic system by altering food prices and so affecting food demand, nutrition, and human livelihoods (Herrero et al., 2010). We have already shown that season-to-season variability in rainfall is high, and the distribution of rainfall in addition to the total is of paramount importance to Kenyan agriculture. In Kenya, declines in per capita maize production have been reported for certain regions (Funk, Davenport, et al., 2018). Much of this change is due to variable seasonal rainfall and the incidence of crop failure. Our results are consistent with work that projects reduced rainfed maize yields in Kenya (Herrero et al., 2010; Thornton et al., 2010). While yield gains have been projected for certain highland areas in the temperate areas of Kenya (Thornton et al., 2010), farmers in the semiarid and arid lowlands are predicted to experience diminished yields, likely forcing them to sow varieties with shorter maturity periods.

In order to capitalize on any potential yield increases in the highlands and reduce as much as possible the decreased yields in the majority of Kenya, further investment in new varieties, improved inputs, and services will be needed (Hansen et al., 2011; Herrero et al., 2010). Investing in varieties that conserve root-zone soil moisture or have deeper roots may be especially important in a warming climate (Rigden et al., 2020). Access to irrigation and water harvesting more generally will be an important way for farmers to buffer negative climate impacts. In this region in central Kenya, access to irrigation resources is not ubiquitous and even those farmers with access to irrigation experience high spatial and temporal variability in its availability (Gower et al., 2016). McCord et al. (2018) show that farmers in the Mount Kenya region with greater relative variability in water flow from irrigation are more likely to uptake adaptation measures such as choosing new seed varieties. This is a positive indication that perhaps the agriculturalists who are more impacted by rainfall variability due to reduced irrigation access are likely to employ adaptation measures or at least experiment with those measures such as changing to an early or extra-early maturing varieties (McCord et al., 2018).

#### 4.4. Study Limitations and Future Research

We made some important assumptions in our model, a common practice in such studies (e.g., Challinor et al., 2009; Tesfaye et al., 2016). First, other than the rainfall climatology and the crop coefficient all other variables such as temperature, carbon dioxide effects and vapor pressure deficit were held constant. All of these variables could markedly affect the relationship between rainfall and crop yields and warrant future

investigation. We do not simulate the effect of inputs such as fertilizer application or irrigation use. The model assumes that nutrients like nitrogen are available in adequate quantities that do not limit growth crop and yield. Second, we do not simulate other crops which might be intercropped with maize (e.g., beans, potatoes), and we do not simulate crop rotation or varying cropping densities. Additional studies may begin with any of these assumptions to further evaluate their effects on maize production.

Future studies would benefit from adding empirical agronomic or decision-making data as inputs or validation datasets. Our study has shown that available water content is lowest during the latter part of the season when the crop coefficient is the highest and the rainfall slackens. A follow-up study could investigate the intra-seasonal nature of water stress to demonstrate what duration of stress during the season makes the largest impact in terms of yield. To answer this question, an empirical data set is needed that includes both intra-seasonal stress dynamics and end of season yields. Additionally, we did not constrain the behavior of early, medium, and late maturing varieties other than changing the length of their growing periods. Early maturing maize is often bred or genetically modified to be drought tolerant and thus should reduce the probability of crop failure. These constraints could be added as parameters in the dynamic water stress calculation or by altering the crop coefficient for hybrid maturities. Field-collected data or on-farm trials would be needed to constrain these parameters.

## 5. Conclusions

This stochastic ecohydrological model represents conditions that will become more common as climate variability and climate change alters rainfall in tropical and semiarid systems. By using historical rainfall to generate stochastic conditions for average depth and probability of rainfall we simulated a dryland environment for small-scale producers. We considered a common crop choice (maize), soil type, and planting decisions (i.e., timing of planting) that represents hundreds of millions of small-scale producers in regions vulnerable to climate change and variability. We investigated the role of rainfall variability in explaining current and past agricultural outcomes such as yield and likelihood of total crop failure. Additionally, we show the importance of cultivar choice in determining yield potentials and the vulnerability of late maturing varieties to rainfall variability. The large divergence in farmer outcomes at low seasonal rainfall totals is concerning. The within season characteristics of how and when rainfall occurs creates the water stress environment that leads to crop failure in some cases and relatively high yields in others.

While process-based and terrestrial biosphere models can simulate hydrological processes and phenology to answer questions about the effects on climate variability on crop outcomes, our research furthers the field of simple stochastic ecohydrological models in which hydrologic processes are often considered separate from the phenology of the crop. We defined water availability as a function of stochastic rainfall and soil parameters whereas the crop coefficient governed water demand. Our model especially considers the rainfall depth and frequency ( $\alpha$  and  $\lambda$ ) parameters as forces that drive stochastic rainfall. Thus we can simulate time-varying soil moisture which changes over the course of the season due to shifts in the water required by the crop and changing rainfall statistics.

In the face of climate change, where direct changes in water availability, temperature, and increased prevalence of pest and diseases are possible, farmers can adapt through two key management strategies: choice of cultivar maturities and planting dates (Van Ittersum et al., 2013). Farmers need to select locally relevant planting dates and cultivars with appropriate maturities to minimize crop failure. Future study on the role of planting dates would illuminate the relative advantages of early to late maturing crops planted during Kenya's two primary rainy seasons. With appropriate climate data and locally relevant agronomic conditions, this type of modeling can be used as a heuristic to improve our understanding of the impacts of climate variability on farming outcomes in other contexts.

## Appendix A: Uncertainties in Maximum Yields

We use seed company-provided estimates of hybrid maize yields to set maximum values of yields by maturity period. These values should be considered as the "potential yields" for a given variety because they are usually attained from optimal growing conditions and from the possible addition of agricultural inputs

and management (fertilizer, weeding, etc.) that does not necessarily reflect small-scale farming conditions (Blekking et al., 2021). How to ascertain whether seed company-provided yields can actually be attained is through cultivar trials, which are done through local research stations that play an important role in certifying seeds and verifying seed company reported yields. Blekking et al. (2021) compared yields between maize companies, Zambia's Seed Control and Certification Institute (SCCI) and from smallholder farms for five varieties in Zambia during the 2011/12 growing season. They found that the seed developer stated potential yields, average yields verified through SCCI cultivar trials, and farmer yields differed vastly. Farmer yields were just a third or less than the company stated yields.

For the hybrid varieties of interest in our study, the range of maximum yields was roughly 1.5 to 5 t/ha as shown in Figure 3. However, our model simulations which were subjected to stochastic rainfall resulted in lower average yields with averages between 1.18 and 1.45 for early to late maturing crops (Table 5). Previous work has shown that regional yields vary and were an average of 0.92–1.55 t/ha between 2000 and 2014 in Laikipia county (Davenport et al., 2019). Given this information, our simulated maize yields fall within regional maize yields. Despite the differences seen between seed company yields and realized yields (Blekking et al., 2021) our model results align with some of the regional yields typically seen for our study site. Future work could better tune the realized yields for a range of maturity periods to better simulate the typical yields found at small-scale farms.

## Appendix B: Sensitivity Analysis

We conducted a sensitivity analysis to investigate whether model parameters related to static and dynamic water stress and evaporation affect the model results. These four variables ( $r$ ,  $k$ ,  $q_e$ , and  $q_{stress}$ ) are interlinked and difficult to measure directly. We find that yields are particularly sensitive to the value of  $k$  in affecting the range of yields, median yield value, and likelihood of crop failure. The value of  $r$  also changes the range of yields but has a limited affect on the median yield. We settled on  $r = 0.5$  as our value because Porporato et al. (2001) selected this response between stress and yield to be less than linear (i.e., the square root of the term). The  $k$  parameter has the opposite effect where smaller values of  $k$  lead to lower yields whereas higher values lead to higher yields. The  $k$  parameter is the portion of the season that the crop can tolerate stress before it fails. Both of these values are interlinked with the calculations of dynamic stress and therefore end of season yields, and are tied to the crop's physiology. Our results show that these values impact the model results and therefore more data is needed on how intra-seasonal water availability affects the duration and severity of stress and therefore crop outcomes. These values are both difficult to resolve among variety types and are difficult to disentangle since they are both tied to the crop's physiology. Thus very little data exists on the effects of intraseasonal crop stress on yield outcomes. Crop modeling studies often only work with seasonal rainfall totals or average weather rather than within season rainfall variability. Increased attention needs to be paid to these parameters which would be improved through field trials and real-time estimates of crop growth under varying meteorological conditions.

Sensitivity Analyses

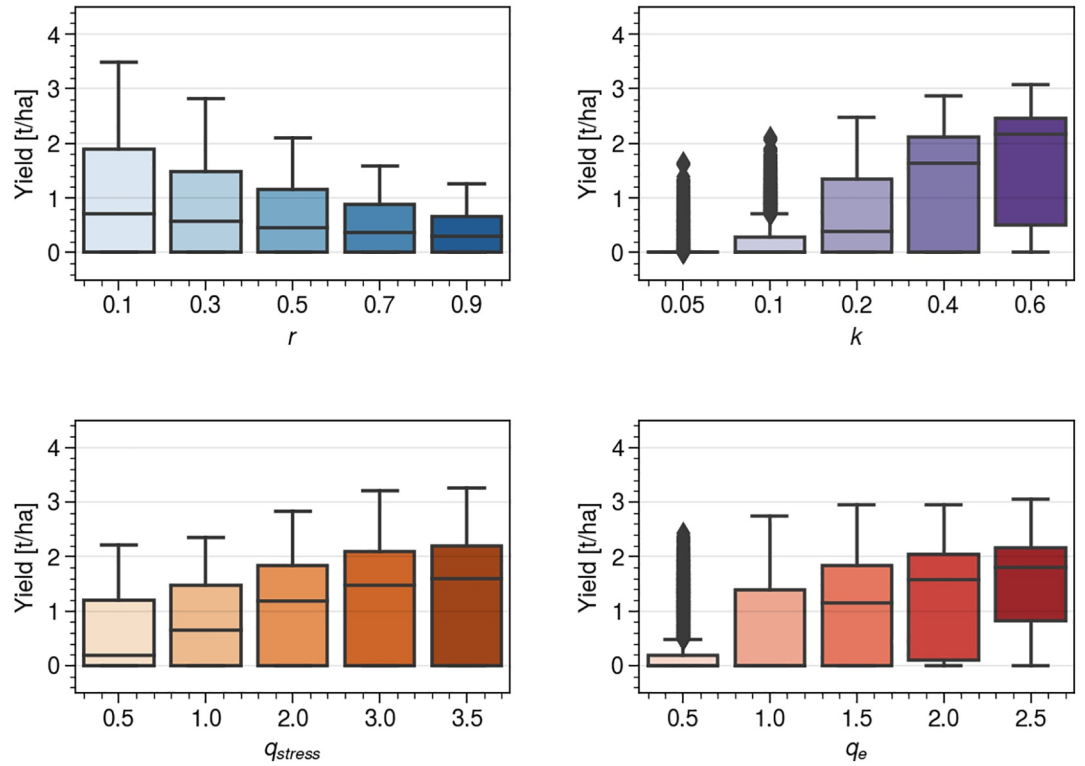
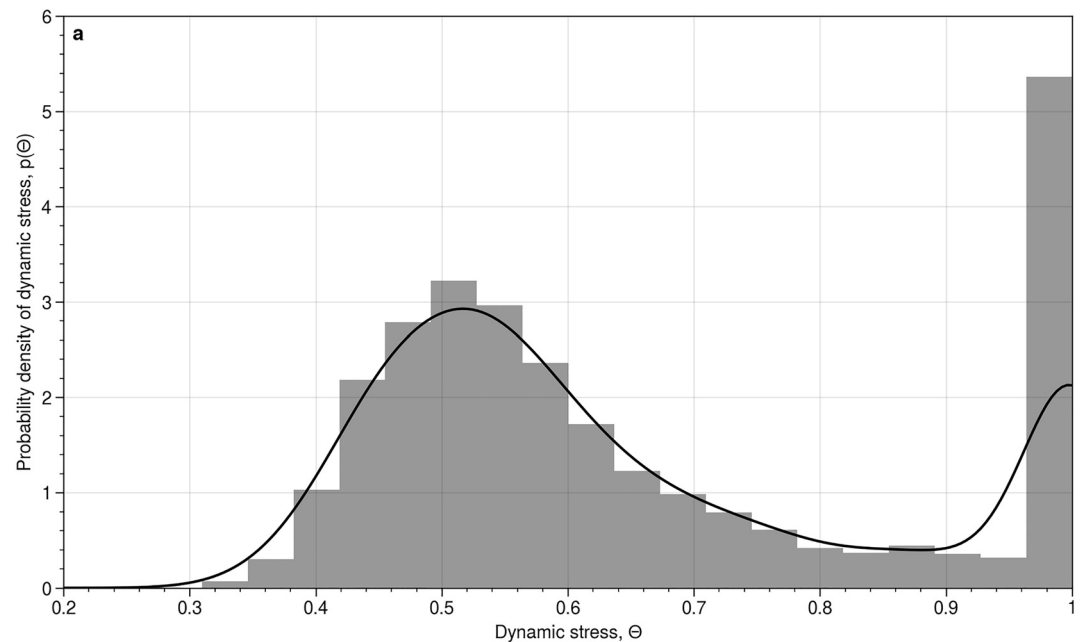


Figure B1. Effect of different values of  $r$ ,  $k$ ,  $q_{stress}$  and  $q_e$  on yields.

### Appendix C: PDF of Dynamic Stress



**Figure C1.** Probability distribution function of dynamic water stress for 10,000 simulations. Model parameters used are the same as those in Figure 6.

### Appendix D: Rainfall-Yield Relationships for Varieties

There is a wide range of yields and therefore farmer outcomes associated with certain bands of rainfall as shown in Figure D1. In the early maturing varieties, we are concerned about the divergence of yield outcomes within the band of 100–200 mm of seasonal rainfall; 150–300 mm of rainfall for medium maturing, and 200–400 mm of rainfall for late maturing. For these bands of rainfall, we find that a wide range of outcomes are possible for farmers such that one farmer (i.e., one model realization) that experiences 175 mm of seasonal rainfall for an early maturing variety can realize about 75 percent of the crop's maximum yield while another farmer that receives 175 mm of rainfall experiences total crop failure. We find this relationship across all of the varieties categories in which some realizations get no yield or very little yields while others get 50–75 percent of their maximum yield for the same seasonal rainfall total. The only difference between these two outcomes (no yield vs. decent yield) is the timing of rainfall because the total rainfall is the same.



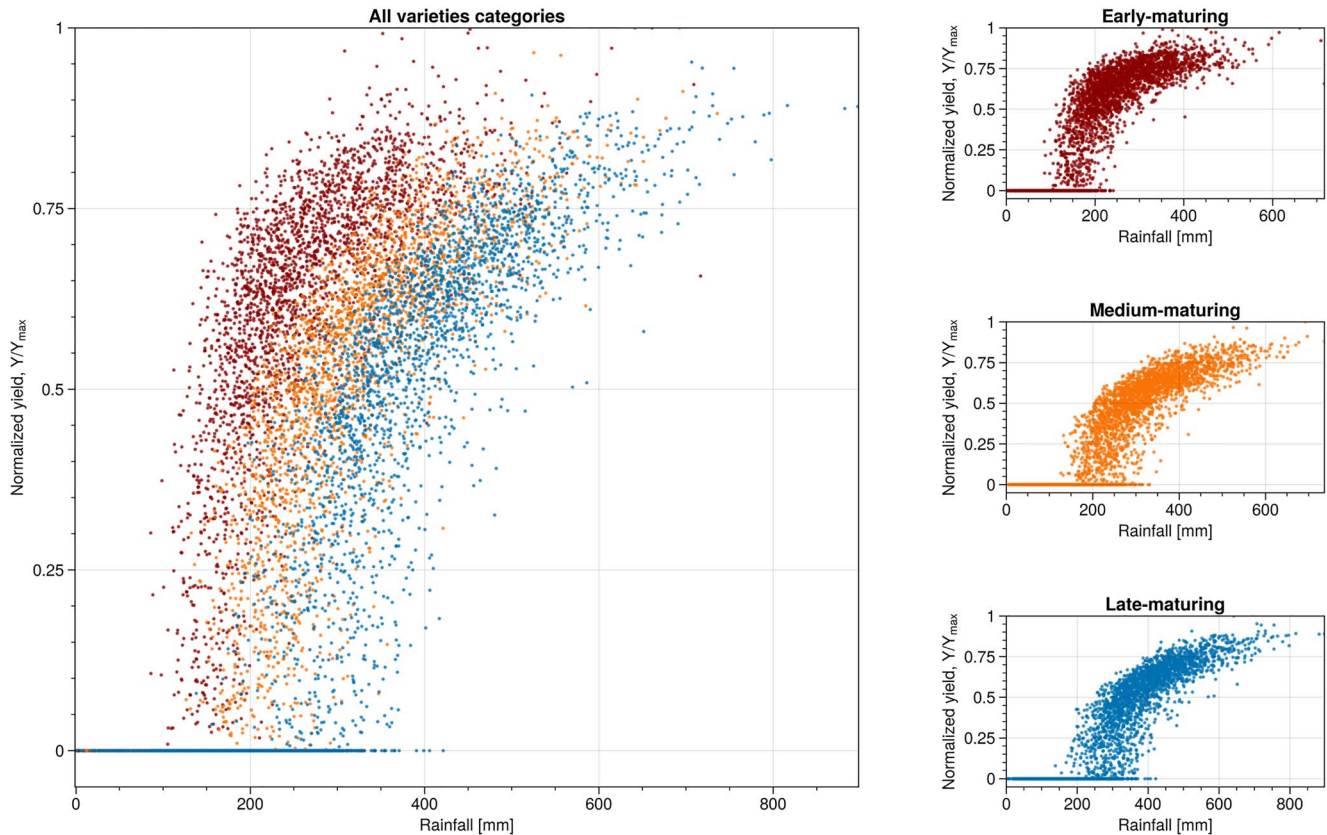


**Figure D1.** Relationships between seasonal rainfall and normalized yields for three categories of varieties: Early maturing (red), Medium maturing (orange), and Late maturing (blue).

### Data Availability Statement

The model output data that support the findings of the study are available on the Github repository <https://doi.org/10.5281/zenodo.5204423>. CETRAD in Nanyuki, Kenya provided us with the historical rain gauge data set.

### Acknowledgments

Noah Spahn provided consultations to improve computational efficiency in the model. The research was supported by the National Science Foundation grants SES-1801251, SES-1360421, and DEB-1924309.

### References

- Allen, R., Pereira, L., Raes, D., & Smith, M. (1998). *Chapter 6-etc-single crop coefficient (kc). Crop evapotranspiration—guidelines for computing crop water requirements—FAO irrigation and drainage paper 56*.
- Apurv, T., Sivapalan, M., & Cai, X. (2017). Understanding the role of climate characteristics in drought propagation. *Water Resources Research*, 53(11), 9304–9329. <https://doi.org/10.1002/2017wr021445>
- Barron, J., Rockström, J., Gichuki, F., & Hatibu, N. (2003). Dry spell analysis and maize yields for two semi-arid locations in east Africa. *Agricultural and Forest Meteorology*, 117(1–2), 23–37. [https://doi.org/10.1016/s0168-1923\(03\)00037-6](https://doi.org/10.1016/s0168-1923(03)00037-6)
- Baudena, M., Boni, G., Ferraris, L., von Hardenberg, J., & Provenzale, A. (2007). Vegetation response to rainfall intermittency in drylands: Results from a simple ecohydrological box model. *Advances in Water Resources*, 30(5), 1320–1328. <https://doi.org/10.1016/j.advwatres.2006.11.006>
- Bharwani, S., Bithell, M., Downing, T. E., New, M., Washington, R., & Ziervogel, G. (2005). Multi-agent modelling of climate outlooks and food security on a community garden scheme in Limpopo, South Africa. *Philosophical Transactions of the Royal Society of London B Biological Sciences*, 360(1463), 2183–2194. <https://doi.org/10.1098/rstb.2005.1742>
- Blekking, J., Waldman, K. B., & Evans, T. (2021). Hybrid-maize seed certification and smallholder adoption in Zambia. *Journal of Environmental Planning and Management*, 64(2), 359–377. <https://doi.org/10.1080/09640568.2020.1764342>
- Branca, G., McCarthy, N., Lipper, L., Jolejole, M. C., & et al. (2011). Climate-smart agriculture: A synthesis of empirical evidence of food security and mitigation benefits from improved cropland management. *Mitigation of climate change in agriculture series*, 3, 1–42.
- Caylor, K. K., Manfreda, S., & Rodriguez-Iturbe, I. (2005). On the coupled geomorphological and ecohydrological organization of river basins. *Advances in Water Resources*, 28(1), 69–86. <https://doi.org/10.1016/j.advwatres.2004.08.013>
- Challinor, A. J., Ewert, F., Arnold, S., Simelton, E., & Fraser, E. (2009). Crops and climate change: Progress, trends, and challenges in simulating impacts and informing adaptation. *Journal of Experimental Botany*, 60(10), 2775–2789. <https://doi.org/10.1093/jxb/erp062>

- Choi, H. S., Schneider, U. A., Rasche, L., Cui, J., Schmid, E., & Held, H. (2015). Potential effects of perfect seasonal climate forecasting on agricultural markets, welfare and land use: A case study of Spain. *Agricultural Systems*, *133*, 177–189. <https://doi.org/10.1016/j.agry.2014.10.007>
- Christensen, J., Hewitson, B., Busuioc, A., Chen, A., Gao, X., Held, I., & Whetton, P. (2007). Regional climate projections. In S. Solomon, et al. (Eds.), *Climate change 2007: The physical science basis. Contribution of working group I to the fourth assessment report of the intergovernmental panel on climate change*. Cambridge, UK: Cambridge University Press.
- Clapp, R. B., & Hornberger, G. M. (1978). Empirical equations for some soil hydraulic properties. *Water Resources Research*, *14*(4), 601–604. <https://doi.org/10.1029/wr014i004p0601>
- Davenport, F. M., Harrison, L., Shukla, S., Husak, G., Funk, C., & McNally, A. (2019). Using out-of-sample yield forecast experiments to evaluate which Earth observation products best indicate end of season maize yields. *Environmental Research Letters*, *14*(12), 124095. <https://doi.org/10.1088/1748-9326/ab5ccd>
- Dinar, A., Hassan, R., Mendelsohn, R., & Benhin, J. (2008). *Climate change and agriculture in Africa: Impact assessment and adaptation strategies*. Routledge.
- Donat, M. G., Lowry, A. L., Alexander, L. V., O’Gorman, P. A., & Maher, N. (2016). More extreme precipitation in the world’s dry and wet regions. *Nature Climate Change*, *6*(5), 508–513. <https://doi.org/10.1038/nclimate2941>
- Downing, T. E., Ringius, L., Hulme, M., & Waughray, D. (1997). Adapting to climate change in Africa. *Mitigation and Adaptation Strategies for Global Change*, *2*(1), 19–44. <https://doi.org/10.1007/bf02437055>
- Erenstein, O., Kassie, G. T., Langyintuo, A. S., & Mwangi, W. (2011). *Characterization of maize producing households in drought prone regions of Eastern Africa*. CIMMYT.
- Fatichi, S., Ivanov, V. Y., & Caporali, E. (2011). Simulation of future climate scenarios with a weather generator. *Advances in Water Resources*, *34*(4), 448–467. <https://doi.org/10.1016/j.advwatres.2010.12.013>
- Franz, T. E., Caylor, K. K., Nordbotten, J. M., Rodríguez-Iturbe, I., & Celia, M. A. (2010). An ecohydrological approach to predicting regional woody species distribution patterns in dryland ecosystems. *Advances in Water Resources*, *33*(2), 215–230. <https://doi.org/10.1016/j.advwatres.2009.12.003>
- Funk, C., & Brown, M. (2009). Declining global per capita agricultural production and warming oceans threaten food security. *Food Security*, *1*(3), 271–289. <https://doi.org/10.1007/s12571-009-0026-y>
- Funk, C., Davenport, F., Eilerts, G., Nourey, N., & Galu, G. (2018). *Contrasting Kenyan resilience to food insecurity: 2011 and 2017*. Tech. Rep. Washington D.C.: Famine Early Warning Systems Network Report, USAID.
- Funk, C., Harrison, L., Shukla, S., Pomposi, C., Galu, G., Korecha, D., et al. (2018). Examining the role of unusually warm Indo-Pacific sea-surface temperatures in recent African droughts. *Quarterly Journal of the Royal Meteorological Society*, *144*, 360–383. <https://doi.org/10.1002/qj.3266>
- Funk, C., Shukla, S., Thiaw, W. M., Rowland, J., Hoell, A., McNally, A., et al. (2019). Recognizing the famine early warning systems network: Over 30 years of drought early warning science advances and partnerships promoting global food security. *Bulletin of the American Meteorological Society*, *100*(6), 1011–1027. <https://doi.org/10.1175/bams-d-17-0233.1>
- Government of Kenya (2010). *Agricultural sector development strategy, 2010-2020*. Government of Kenya.
- Gower, D. B., Dell’Angelo, J., McCord, P. F., Caylor, K. K., & Evans, T. P. (2016). Modeling ecohydrological dynamics of smallholder strategies for food production in dryland agricultural systems. *Environmental Research Letters*, *11*(11), 115005. <https://doi.org/10.1088/1748-9326/11/11/115005>
- Guan, K., Sultan, B., Biasutti, M., Baron, C., & Lobell, D. B. (2017). Assessing climate adaptation options and uncertainties for cereal systems in West Africa. *Agricultural and Forest Meteorology*, *232*, 291–305. <https://doi.org/10.1016/j.agrformet.2016.07.021>
- Guido, Z., Zimmer, A., Lopus, S., Hannah, C., Gower, D., Waldman, K., et al. (2020). Farmer forecasts: Impacts of seasonal rainfall expectations on agricultural decision-making in Sub-Saharan Africa. *Climate Risk Management*, *30*, 100247. <https://doi.org/10.1016/j.crm.2020.100247>
- Hansen, J. W., Mason, S. J., Sun, L., & Tall, A. (2011). Review of Seasonal Climate Forecasting for Agriculture in Sub-Saharan Africa (Vol. 47). <https://doi.org/10.1017/s0014479710000876>
- Harrison, L., Funk, C., & Peterson, P. (2019). Identifying changing precipitation extremes in Sub-Saharan Africa with gauge and satellite products. *Environmental Research Letters*, *14*(8), 085007. <https://doi.org/10.1088/1748-9326/ab2cae>
- Herrero, M., Ringler, C., van de Steeg, J., Thornton, P. K., Zhu, T., Bryan, E., & Notenbaert, A. M. O. (2010). *Climate variability and climate change and their impacts on Kenya’s agricultural sector*. ILRI.
- IPCC. (2007). *Synthesis report. Contribution of working groups i, ii and iii to the fourth assessment report of the intergovernmental panel on climate change*. Geneva, Switzerland: IPCC.
- Kalanda-Joshua, M., Ngongondo, C., Chipeta, L., & Mpembeka, F. (2011). Integrating indigenous knowledge with conventional science: Enhancing localised climate and weather forecasts in Nessa, Mulanje, Malawi. *Physics and Chemistry of the Earth*, *36*(14–15). <https://doi.org/10.1016/j.pce.2011.08.001>
- Katul, G., Porporato, A., & Oren, R. (2007). Stochastic dynamics of plant-water interactions. *Annual Review of Ecology, Evolution and Systematics*, *38*, 767–791. <https://doi.org/10.1146/annurev.ecolsys.38.091206.095748>
- Katz, R. W., & Parlange, M. B. (1998). Overdispersion phenomenon in stochastic modeling of precipitation. *Journal of Climate*, *11*(4), 591–601. [https://doi.org/10.1175/1520-0442\(1998\)011<0591:opismo>2.0.co;2](https://doi.org/10.1175/1520-0442(1998)011<0591:opismo>2.0.co;2)
- Kipkemoi, I., Michaelides, K., Rosolem, R., & Singer, M. B. (2021). Climatic expression of rainfall on soil moisture dynamics in drylands. *Hydrology and Earth System Sciences Discussions*, 1–24.
- Laio, F., Porporato, A., Fernandez-Illescas, C. P., & Rodríguez-Iturbe, I. (2001). Plants in water-controlled ecosystems: Active role in hydrologic processes and response to water stress: IV. Discussion of real cases. *Advances in Water Resources*, *24*(7), 745–762. [https://doi.org/10.1016/s0309-1708\(01\)00007-0](https://doi.org/10.1016/s0309-1708(01)00007-0)
- Laio, F., Porporato, A., Ridolfi, L., & Rodríguez-Iturbe, I. (2001). Plants in water-controlled ecosystems: Active role in hydrologic processes and response to water stress: II. Probabilistic soil moisture dynamics. *Advances in Water Resources*, *24*(7), 707–723. [https://doi.org/10.1016/s0309-1708\(01\)00005-7](https://doi.org/10.1016/s0309-1708(01)00005-7)
- Leenaars, J. (2014). *Africa soil profiles database, version 1.2. A compilation of geo-referenced and standardized legacy soil profile data for Sub-Saharan Africa (with dataset)*. (Wageningen, the Netherlands: Africa Soil Information Service (AfSIS) project and ISRIC—World Soil Information.). Retrieved from <https://data.isric.org/geonetwork/srv/eng/catalog.search#/metadata/2a7d2fb8-e0db-4a4b-9661-4809865aacff>
- Liebmann, B., Hoerling, M. P., Funk, C., Bladé, I., Dole, R. M., Allured, D., et al. (2014). Understanding recent eastern Horn of Africa rainfall variability and change. *Journal of Climate*, *27*(23), 8630–8645. <https://doi.org/10.1175/jcli-d-13-00714.1>
- Liniger, H., & Thomas, D. B. (1998). Grass: Ground cover for restoration of arid and semi-arid soils. *Advances In Geocology*, *31*, 1167–1178.

- Liniger, H., & Weingartner, R. (1998). *Mountains and freshwater supply*. Unasylva (FAO).
- Lobell, D. B., Schlenker, W., & Costa-Roberts, J. (2011). Climate trends and global crop production since 1980. *Science*, 333, 1204531.
- Lyon, B., & DeWitt, D. G. (2012). A recent and abrupt decline in the East African long rains. *Geophysical Research Letters*, 39(2), L02702. <https://doi.org/10.1029/2011gl050337>
- Mahfouf, J.-F., & Jacquemin, B. (1989). A study of rainfall interception using a 1 and surface parameterization for mesoscale meteorological models. *Journal of Applied Meteorology and Climatology*, 28(12), 1282–1302. [https://doi.org/10.1175/1520-0450\(1989\)028<1282:asoriu>2.0.co;2](https://doi.org/10.1175/1520-0450(1989)028<1282:asoriu>2.0.co;2)
- McCord, P., Waldman, K., Baldwin, E., Dell'Angelo, J., & Evans, T. (2018). Assessing multi-level drivers of adaptation to climate variability and water insecurity in smallholder irrigation systems. *World Development*, 108, 296–308. <https://doi.org/10.1016/j.worlddev.2018.02.009>
- Meehl, G. A., Stocker, T. F., Collins, W. D., Friedlingstein, P., Gaye, A. T., Gregory, J. M., et al. (2007). *Global climate projections. Climate change 2007: The physical science basis. Contribution of working group I to the fourth assessment report of the intergovernmental panel on climate change*. Cambridge: Cambridge University Press.
- Morris, M. (2001). *Assessing the benefits of international maize breeding research: An overview of the global maize impacts study. Part II of the CIMMYT 1999–2000 world maize facts and trends*. Tech. Rep. Mexico City: CIMMYT.
- Muchena, F., & Gachene, C. (1988). Soils of the highland and mountainous areas of Kenya with special emphasis on agricultural soils. *Mountain Research and Development*, 8, 183–191. <https://doi.org/10.2307/3673446>
- Müller, C., Cramer, W., Hare, W. L., & Lotze-Campen, H. (2011). Climate change risks for African agriculture. *Proceedings of the National Academy of Sciences of the United States of America*, 108(11), 4313–4315. <https://doi.org/10.1073/pnas.1015078108>
- Neumann, P. M. (2008). Coping mechanisms for crop plants in drought-prone environments. *Annals of Botany*, 101(7), 901–907. <https://doi.org/10.1093/aob/mcn018>
- Nicholson, S. E. (2017). Climate and climatic variability of rainfall over eastern Africa. *Reviews of Geophysics*, 55(3), 590–635. <https://doi.org/10.1002/2016rg000544>
- Nyakudya, I. W., & Stroosnijder, L. (2014). Effect of rooting depth, plant density and planting date on maize (*Zea mays* L.) yield and water use efficiency in semi-arid Zimbabwe: Modelling with AquaCrop. *Agricultural Water Management*, 146, 280–296. <https://doi.org/10.1016/j.agwat.2014.08.024>
- Patakamuri, S. K., & O'Brien, N. (2020). *modifiedmk: Modified versions of mann kendall and spearman's rho trend tests [Computer software manual]*. Retrieved from [https://CRAN.R-project.org/package=modifiedmk\(Rpackageversion1.5.0](https://CRAN.R-project.org/package=modifiedmk(Rpackageversion1.5.0)
- Patt, A., Suarez, P., & Gwata, C. (2005). Effects of seasonal climate forecasts and participatory workshops among subsistence farmers in Zimbabwe. *Proceedings of the National Academy of Sciences of the United States of America*, 102(35), 12623–12628. <https://doi.org/10.1073/pnas.0506125102>
- Porporato, A., D'Odorico, P., Laio, F., Ridolfi, L., & Rodríguez-Iturbe, I. (2002). *Ecohydrology of water-controlled ecosystems* (Vol 25). [https://doi.org/10.1016/s0309-1708\(02\)00058-1](https://doi.org/10.1016/s0309-1708(02)00058-1)
- Porporato, A., Laio, F., Ridolfi, L., Caylor, K. K., & Rodríguez-Iturbe, I. (2003). Soil moisture and plant stress dynamics along the Kalahari precipitation gradient. *Journal of Geophysical Research*, 108(D3), 4127. <https://doi.org/10.1029/2002jd002448>
- Porporato, A., Laio, F., Ridolfi, L., & Rodríguez-Iturbe, I. (2001). Plants in water-controlled ecosystems: Active role in hydrologic processes and response to water stress: III. Vegetation water stress. *Advances in Water Resources*, 24(7), 725–744. [https://doi.org/10.1016/s0309-1708\(01\)00006-9](https://doi.org/10.1016/s0309-1708(01)00006-9)
- Ray, D. K., Gerber, J. S., Macdonald, G. K., & West, P. C. (2015). Climate variation explains a third of global crop yield variability. *Nature Communications*, 6, 1–9. <https://doi.org/10.1038/ncomms6989>
- Ray, D. K., Ramankutty, N., Mueller, N. D., West, P. C., & Foley, J. A. (2012). Recent patterns of crop yield growth and stagnation. *Nature Communications*, 3, 1293. <https://doi.org/10.1038/ncomms2296>
- Recha, C., Makokha, G., Traore, P., Shisanya, C., Lodoun, T., & Sako, A. (2012). Determination of seasonal rainfall variability, onset and cessation in semi-arid Tharaka district, Kenya. *Theoretical and Applied Climatology*, 108(3–4), 479–494. <https://doi.org/10.1007/s00704-011-0544-3>
- Reidsma, P., Ewert, F., Lansink, A. O., & Leemans, R. (2010). Adaptation to climate change and climate variability in European agriculture: The importance of farm level responses. *European Journal of Agronomy*, 32(1), 91–102. <https://doi.org/10.1016/j.eja.2009.06.003>
- Rigden, A., Mueller, N., Holbrook, N., Pillai, N., & Huybers, P. (2020). Combined influence of soil moisture and atmospheric evaporative demand is important for accurately predicting US maize yields. *Nature Food*, 1(2), 127–133. <https://doi.org/10.1038/s43016-020-0028-7>
- Roche, K. R., Müller-Itten, M., Dralle, D. N., Bolster, D., & Müller, M. F. (2020). Climate change and the opportunity cost of conflict. *Proceedings of the National Academy of Sciences of the United States of America*, 117(4), 1935–1940. <https://doi.org/10.1073/pnas.1914829117>
- Rodríguez-Iturbe, I., & Porporato, A. (2007). *Ecohydrology of water-controlled ecosystems: Soil moisture and plant dynamics*. Cambridge University Press.
- Rodríguez-Iturbe, I., Porporato, A., Laio, F., & Ridolfi, L. (2001). Plants in water-controlled ecosystems: Active role in hydrologic processes and response to water stress: I. Scope and general outline. *Advances in Water Resources*, 24(7), 695–705. [https://doi.org/10.1016/s0309-1708\(01\)00004-5](https://doi.org/10.1016/s0309-1708(01)00004-5)
- Roudier, P., Muller, B., d'Aquino, P., Roncoli, C., Soumaré, M. A., Batté, L., & Sultan, B. (2014). The role of climate forecasts in smallholder agriculture: Lessons from participatory research in two communities in Senegal. *Climate Risk Management*, 2, 42–55. <https://doi.org/10.1016/j.crm.2014.02.001>
- Sah, R., Chakraborty, M., Prasad, K., Pandit, M., Tudu, V., Chakravarty, M., & Moharana, D. (2020). Impact of water deficit stress in maize: Phenology and yield components. *Scientific Reports*, 10(1), 1–15. <https://doi.org/10.1038/s41598-020-59689-7>
- Salgado-Aguilar, M., Molnar, T., Pons-Hernández, J. L., Covarrubias-Prieto, J., Ramirez-Pimentel, J. G., Raya-Pérez, J. C., & Iturriaga, G. (2020). Physiological and biochemical analyses of novel drought-tolerant maize lines reveal osmoprotectant accumulation at silking stage. *Chilean Journal of Agricultural Research*, 80(2), 241–252. <https://doi.org/10.4067/s0718-58392020000200241>
- Samberg, L. H., Gerber, J. S., Ramankutty, N., Herrero, M., & West, P. C. (2016). Subnational distribution of average farm size and smallholder contributions to global food production. *Environmental Research Letters*, 11(12), 124010. <https://doi.org/10.1088/1748-9326/11/12/124010>
- Schmocker, J., Liniger, H., Ngeru, J., Brugnara, Y., Auchmann, R., & Brönnimann, S. (2016). Trends in mean and extreme precipitation in the Mount Kenya region from observations and reanalyses. *International Journal of Climatology*, 36(3), 1500–1514. <https://doi.org/10.1002/joc.4438>
- Senay, G. (2004). *Crop Water Requirement Satisfaction Index (WRSI) model description*.
- Setimela, P. S., Magorokosho, C., Lunduka, R., Gasura, E., Makumbi, D., Tarekne, A., et al. (2017). On-farm yield gains with stress-tolerant maize in Eastern and Southern Africa. *Agronomy Journal*, 109(2), 406–417. <https://doi.org/10.2134/agronj2015.0540>

- Shongwe, M. E., van Oldenborgh, G. J., van den Hurk, B., & van Aalst, M. (2011). Projected changes in mean and extreme precipitation in Africa under global warming. Part II: East Africa. *Journal of Climate*, *24*(14), 3718–3733. <https://doi.org/10.1175/2010jcli2883.1>
- Singer, M. B., & Michaelides, K. (2017). Deciphering the expression of climate change within the Lower Colorado River basin by stochastic simulation of convective rainfall. *Environmental Research Letters*, *12*(10), 104011. <https://doi.org/10.1088/1748-9326/aa8e50>
- Slingo, J. M., Challinor, A. J., Hoskins, B. J., & Wheeler, T. R. (2005). Introduction: Food crops in a changing climate. *Philosophical Transactions of the Royal Society of London B Biological Sciences*, *360*(1463), 1983–1989. <https://doi.org/10.1098/rstb.2005.1755>
- Smale, M., & Jayne, T. S. (2010). 'seeds of success' in retrospect: Hybrid maize in Eastern and Southern Africa. *Successes in African Agriculture: Lessons for the Future* (Vol. 71–112).
- Taylor, R. G., Todd, M. C., Kongola, L., Maurice, L., Nahozya, E., Sanga, H., & MacDonald, A. M. (2013). Evidence of the dependence of groundwater resources on extreme rainfall in East Africa. *Nature Climate Change*, *3*(4), 374–378. <https://doi.org/10.1038/nclimate1731>
- Tesfaye, K., Sonder, K., Caims, J., Magorokosho, C., Tarekegn, A., Kassie, G. T., & Erenstein, O. (2016). Targeting drought-tolerant maize varieties in Southern Africa: A geospatial crop modeling approach using big data. *International Food and Agribusiness Management Review IFAMA*, *19*, 75–92.
- Thornton, P. K., Jones, P. G., Alagarswamy, G., Andresen, J., & Herrero, M. (2010). Adapting to climate change: Agricultural system and household impacts in East Africa. *Agricultural Systems*, *103*(2), 73–82. <https://doi.org/10.1016/j.agsy.2009.09.003>
- Trenberth, K. E. (2011). Changes in precipitation with climate change. *Climate Research*, *47*(1–2), 123–138. <https://doi.org/10.3354/cr00953>
- Van Ittersum, M. K., Cassman, K. G., Grassini, P., Wolf, J., Titttonell, P., & Hochman, Z. (2013). Yield gap analysis with local to global relevance—A review. *Field Crops Research*, *143*, 4–17. <https://doi.org/10.1016/j.fcr.2012.09.009>
- Vervoort, R. W., Willem Vervoort, R., Muita, R., Ampt, P., & van Ogtrop, F. (2016). Managing the water cycle in Kenyan small-scale maize farming systems: Part 2. Farmers' Use of Formal and Informal Climate Forecasts (Vol. 3). <https://doi.org/10.1002/wat2.1121>
- Waldman, K. B., Vergopolan, N., Attari, S. Z., Sheffield, J., Estes, L. D., Caylor, K. K., & Evans, T. P. (2019). Cognitive biases about climate variability in smallholder farming systems in Zambia. *Weather, Climate, and Society*, *11*(2), 369–383. <https://doi.org/10.1175/wcas-d-18-0050.1>
- Wiesmann, U. (1998). *Sustainable regional development in rural Africa: Conceptual framework and case studies from Kenya*. University of Berne Switzerland, Institute of Geography.
- Williams, A. P., & Funk, C. (2011). A westward extension of the warm pool leads to a westward extension of the walker circulation, drying Eastern Africa. *Climate Dynamics*, *37*(11–12), 2417–2435. <https://doi.org/10.1007/s00382-010-0984-y>
- Williams, C. A., & Albertson, J. D. (2004). Soil moisture controls on canopy-scale water and carbon fluxes in an African savanna. *Water Resources Research*, *40*(9), W09302. <https://doi.org/10.1029/2004wr003208>
- Wood, S. A., Jina, A. S., Jain, M., Kristjanson, P., & DeFries, R. S. (2014). Smallholder farmer cropping decisions related to climate variability across multiple regions. *Global Environmental Change*, *25*, 163–172. <https://doi.org/10.1016/j.gloenvcha.2013.12.011>
- Yue, S., & Wang, C. (2004). The mann-kendall test modified by effective sample size to detect trend in serially correlated hydrological series. *Water Resources Management*, *18*(3), 201–218. <https://doi.org/10.1023/b:warm.0000043140.61082.60>
- Zheng, J., Fan, J., Zhang, F., Yan, S., & Xiang, Y. (2018). Rainfall partitioning into throughfall, stemflow and interception loss by maize canopy on the semi-arid loess plateau of china. *Agricultural Water Management*, *195*, 25–36. <https://doi.org/10.1016/j.agwat.2017.09.013>
- Ziervogel, G., Bithell, M., Washington, R., & Downing, T. (2005). Agent-based social simulation: A method for assessing the impact of seasonal climate forecast applications among smallholder farmers. *Agricultural Systems*, *83*(1), 1–26. <https://doi.org/10.1016/j.agsy.2004.02.009>